

NASA TECHNICAL NOTE

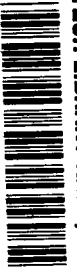


NASA TN D-4102

c.1

LOAN COPY: RETURN
AFWL (WLIL-2)
KIRTLAND AFB, N M

0330995



TECH LIBRARY KAFB, NM

NASA TN D-4102

HELIUM PRESSURANT REQUIREMENTS FOR LIQUID-HYDROGEN EXPULSION USING SUBMERGED GAS INJECTION

by William R. Johnson
Lewis Research Center
Cleveland, Ohio



**HELIUM PRESSURANT REQUIREMENTS FOR LIQUID-HYDROGEN
EXPULSION USING SUBMERGED GAS INJECTION**

By William R. Johnson

Lewis Research Center
Cleveland, Ohio

NATIONAL AERONAUTICS AND SPACE ADMINISTRATION

For sale by the Clearinghouse for Federal Scientific and Technical Information
Springfield, Virginia 22151 - CFSTI price \$3.00

HELIUM PRESSURANT REQUIREMENTS FOR LIQUID-HYDROGEN EXPULSION USING SUBMERGED GAS INJECTION

by William R. Johnson

Lewis Research Center

SUMMARY

An experimental investigation was conducted to determine the helium pressurant requirements for the expulsion of liquid hydrogen by the direct injection of helium into the liquid. As the helium was bubbled up through the liquid hydrogen, hydrogen was vaporized, diffused into the bubbles, and carried into the ullage volume. The prime purpose of this injection technique was to minimize the amount of helium gas required for expulsion by supplementing the helium with vaporized hydrogen.

The helium pressurant was injected into the 12.6-cubic-foot (0.357 cu m) cylindrical test tank through a porous flat plate formed by layers of screen sintered together. Propellant vaporization by direct heat addition was minimized by (1) injecting the helium at liquid-hydrogen temperature, and (2) locating the test tank in an auxiliary tank filled with liquid hydrogen. Nominal test tank pressures of 21, 25, and 33 psia (145×10^3 , 172×10^3 , and 228×10^3 N/m²) were maintained for expulsions ranging in length from 60 to 300 seconds. The initial temperature of the liquid hydrogen was varied from approximately 36.0° to 38.0° R (20.0° to 21.1° K).

The results of the experimental program showed the helium pressurant to be nearly 100 percent saturated with vaporized hydrogen after expansion into the ullage volume. The degree of saturation obtained was not measurably affected by varying expulsion time, tank pressure level, or initial liquid temperature. Furthermore, the major share of the vaporization and diffusion of hydrogen into the individual helium bubbles occurred immediately upon injection of the bubbles into the liquid. The helium pressurant requirements for the submerged injector were compared analytically with those for a conventional overhead hot-gas injector. The results show that the weight of helium pressurant required for the submerged injection technique is approximately that required for a hot-gas system, but only at low tank pressures and/or low values of NPSP.

INTRODUCTION

One of the prime objectives in optimizing any liquid-hydrogen tank-pressurization system is to minimize the total system weight without sacrificing the reliability of the system. The total system weight contributed by the stored gas, tankage, and hardware required for a given pressurization-system concept must be balanced against the degree of reliability realized with that particular concept. In general, a high degree of reliability can be obtained by reducing the complexity of operation and control of a given system to a minimum.

A cold-gas system that approaches a minimum complexity stores helium gas at liquid-hydrogen temperature (37° R (20.6° K)). The gas is expanded on demand through a conventional overhead injector directly into the propellant tank. For a hot-gas system in which helium is injected through the same overhead injector at an elevated temperature, a heat exchanger with access to a warm fluid, additional lines and valves, and possibly more sophisticated controlling devices must be utilized. The additional hardware required for a hot-gas system adds to the total system weight and also to the overall system complexity, as compared with a cold-gas system.

The apparent gain in reliability of the cold-gas system over the hot-gas system is offset by the increased weight of helium pressurant required for the cold-gas system. The helium pressurant required to expel a given volume of liquid hydrogen at a constant tank pressure is inversely proportional to the final helium gas temperature in the ullage volume (i. e., $W_{\text{GHe}} = P_{\text{GHe}} V_u / z_{\text{GHe}} R_{\text{GHe}} T_u$, the perfect gas law). (All symbols are defined in appendix A.) Injecting the helium pressurant into the propellant tank ullage volume at 37° R (20.6° K) requires the maximum weight of helium pressurant.

However, one means of reducing the weight of helium pressurant required for a cold-gas system involves supplementing the helium in the ullage with vaporized propellant. A technique conceived for maximizing the amount of vaporized hydrogen in the ullage utilizes a submerged helium gas injector. By bubbling the helium gas up through the liquid hydrogen, a greater surface area for evaporation and diffusion of hydrogen into the bubbles can be realized. The hydrogen continues to diffuse into the bubbles until thermodynamic phase equilibrium is reached. The equilibrium point is established when the partial pressure of the hydrogen in the bubble is exactly equal to the saturated vapor pressure of the liquid hydrogen at the particular temperature of the liquid. In essence, the submerged injector fills the ullage volume with a mixture of helium gas and hydrogen vapor. The conventional overhead injector simply fills the ullage volume with practically pure helium gas.

Since several investigators (refs. 1 and 2) previously demonstrated that liquid hydrogen is vaporized and diffused into the injected helium gas bubbles, this investigation was conducted to

- (1) Determine whether this mixture of hydrogen vapor and helium gas can be expanded into the ullage and retained during the expulsion so that a negligible amount of vaporized hydrogen will condense out
- (2) Compare the experimental values of helium pressurant required to the ideal (complete saturation of the ullage with vaporized hydrogen)
- (3) Determine the effect of various physical test variables such as liquid temperature, tank pressure, expulsion rate, and liquid height on the degree of saturation obtained
- (4) Compare analytically the helium pressurant requirements of the submerged injector with those of a hot-gas overhead injector.

APPARATUS

A schematic diagram of the experimental test facility is shown in figure 1. The test tank was suspended in an auxiliary tank equipped with a separate liquid-hydrogen flow system. A liquid-hydrogen bath completely surrounding the test tank was maintained during each experimental data run to

- (1) Minimize the external heat leak into the test tank
- (2) Provide a heat sink for cooling the helium pressurant to liquid-hydrogen temperature before injection into the test tank.

This procedure minimized propellant vaporization by direct heat addition and thus ensured that the net charge in the hydrogen vapor in the ullage volume at any time after the start of expulsion could be attributed to the submerged injection technique.

The external heat leak due to the finite temperature difference between the liquid hydrogen in the bath and that in the test tank was minimized by insulating the exterior surface of the test tank. The cylindrical section of the test tank was covered with two layers of 0.25-inch (0.64 cm) corkboard and then a vapor barrier of 0.005-inch (0.013 cm) polyester film. The test tank lid was covered with a 4-inch (10.2 cm) thickness of urethane plastic foam. The bottom of the test tank was not insulated since heat addition or removal from the liquid hydrogen at this point during the expulsion only changes the temperature of the liquid hydrogen passing through the flowmeter. A platinum resistance thermocouple on the tank bottom, together with the tank pressure measurements, provided data to compute the density of liquid hydrogen passing through the flowmeter.

The helium-pressurant flow rates were measured with calibrated orifice plates located in a region of high pressure (160 psia ($1.1 \times 10^6 \text{ N/m}^2$)) and ambient temperature (520° R (289° K)). The pressurant was cooled to liquid-hydrogen temperature by passing it through eight stainless-steel coils, 50 feet (15.2 m) in length and 1-inch (2.5 cm)

in diameter, located in the hydrogen bath in the auxiliary tank. The helium temperature before injection into the test tank was measured with a platinum resistance thermocouple. A pneumatic flow-control valve activated by a controller sensing tank pressure regulated the helium pressurant flow rate to maintain a set tank pressure throughout the expulsion.

The liquid outflow rate was controlled by a variable flow valve and was measured with a turbine-type flowmeter. The commercially available flowmeter was calibrated with liquid hydrogen prior to installation.

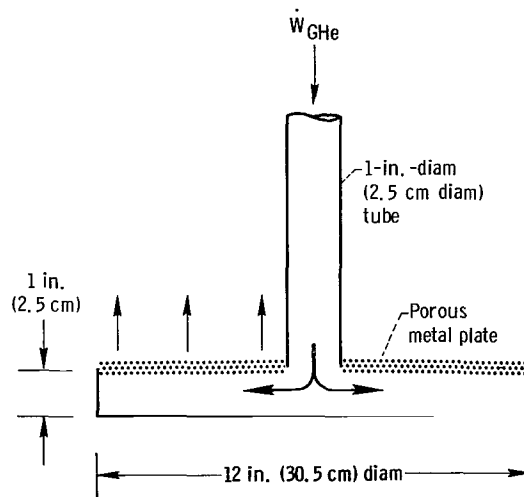
Electrical strip heaters located at the bottom of the test tank enabled different initial propellant temperatures to be obtained.

A schematic diagram of the test tank with the location of the internal instrumentation is shown in figure 2. The test tank has an inner diameter of 21.4 inches (54.4 cm) and a cylindrical length of 57.6 inches (146.3 cm). The tank material is 304 stainless steel with a wall thickness of 0.188 inch (0.478 cm). Two 22-inch-outside-diameter by 4-inch-thick (55.9 cm o. d. by 0.64 cm thick), flanged and dished heads were used as the tank ends.

The vertical temperature rake consists of 12 platinum resistance thermocouples equally spaced 4.75 inches (12.07 cm) apart positioned near the half radius of the tank or 5.7 inches (14.5 cm) from the tank centerline. The horizontal rake consists of four additional platinum resistance thermocouples equally spaced 2.25 inches (5.72 cm) apart. The horizontal rake was located in a plane 1 inch (2.5 cm) above the injector to measure radial temperature gradients.

Three commercially available hot-wire liquid-level sensors were mounted on the vertical rake. The bottom sensor was located 2 inches (5.1 cm) above the injector. The vertical distance between the bottom and top sensors was 50.25 inches (127.64 cm). The middle sensor was positioned exactly midway between the top and bottom sensors. A commercially available optical liquid-level sensor was positioned inside the test tank in the same plane as the top hot-wire sensor to substantiate the hot-wire-sensor reading.

The helium pressurant was injected into the liquid hydrogen through a 12-inch-diameter (30.5 cm diam) porous metal plate, as shown in the sketch. The pressurant was introduced to the enclosed supply cavity by a 1-inch-diameter (2.5 cm diam) tube. The criteria for the selection of the porous plate and the preliminary testing of this material are discussed in detail in appendix B.



ANALYTICAL PROGRAM

General Case - Constant Tank Pressure

The minimum or ideal helium pressurant required for the expulsion of a given volume of liquid hydrogen is realized when the expelled volume has been filled with the maximum amount of hydrogen vapor that is thermodynamically possible. This condition occurs when the partial pressure of hydrogen in the expelled volume is equal to the saturated vapor pressure of hydrogen corresponding to the temperature of the expelled liquid.

The vaporization of hydrogen during the expulsion removes heat from the liquid hydrogen and thus causes the average bulk liquid temperature to decrease with time. This decrease in temperature markedly reduces the saturated vapor pressure of the liquid hydrogen (fig. 3) and thus reduces the partial pressure of hydrogen being supplied to the ullage. If the tank pressure is held constant during the expulsion, the helium pressurant flow rate must increase accordingly, as shown in the following equations:

$$P_{GHV} = f(T_{LH})$$

$$P_{GHe} = P_t - P_{GHV}$$

The rate of evaporation of hydrogen during liquid outflow is proportional to the partial pressure of hydrogen being maintained in the ullage volume segment located immediately above the interface. The quantity of heat removed from the liquid during this time is proportional to the amount vaporized as well as to the temperature at which the liquid is vaporized. The change in temperature of the remaining bulk liquid is dependent on the quantity of heat removed, the specific heat of the liquid, and the quantity of bulk liquid remaining.

Because of the interrelation of the preceding items with respect to a changing bulk liquid temperature, the ideal case could best be determined by an analytical computer program. The following basic assumptions were incorporated in the analysis:

- (1) Complete saturation of the helium bubbles
- (2) No radial temperature gradients (injector face area equal to the cross-sectional area of the test tank)
- (3) No vertical temperature gradients (heat of vaporization removed uniformly from the total mass of liquid above the injector at any given time)
- (4) No ambient heat flux
- (5) No heat flux from the helium pressurant (helium pressurant inlet temperature assumed equal to the changing liquid temperature)

Data input to the program consisted of tank pressure, initial liquid volume above the plane of the injector, and initial average bulk liquid temperature. The thermodynamic properties of hydrogen and helium were obtained from references 3 and 4.

The total volume of liquid hydrogen to be expelled is divided into individual liquid-volume increments, and each increment is considered independently. The ullage volume resulting from the expulsion of each liquid volume increment must include not only the volume of liquid expelled, but also the volume of liquid vaporized and the increase in ullage volume due to the thermal contraction of the remaining liquid. A detailed mathematical analysis of the calculations for any given segment can be found in appendix C. Initial trial runs indicated no significant change in results when the liquid-volume increment was decreased below 0.05 cubic foot (1416 cu cm). On this basis, approximately 200 volume increments constituted a complete expulsion.

The program then calculated the pounds of liquid hydrogen expelled per pound of helium pressurant supplied for a given tank pressure and average liquid temperature. This ratio was determined for each increment, as well as accumulatively throughout the expulsion.

Special Case - Constant Net Positive Suction Pressure

The tank pressure required for a pump-fed vehicle is classically defined as

$$P_t = \text{NPSP} + P_{\text{GHV}} + \frac{\text{Feed-line}}{\text{pressure drop}} - \text{Propellant head}$$

For simplicity, the propellant head and the feed-line pressure drop are included in the net positive suction pressure NPSP term and result in

$$P_t = \text{NPSP} + P_{\text{GHV}}$$

If the NPSP is arbitrarily assumed to be 4 psia ($28 \times 10^3 \text{ N/m}^2$) and the liquid temperature at the pump inlet to be 37.35° R (20.54° K), there results

$$\begin{aligned} P_t = \text{NPSP} + P_{\text{GHV}} &= 4 \text{ psia} + 17 \text{ psia} = 21 \text{ psia} \\ &= 28 \times 10^3 \text{ N/m}^2 + 117 \times 10^3 \text{ N/m}^2 = 145 \times 10^3 \text{ N/m}^2 \end{aligned}$$

However, if the liquid was subcooled to 33° R (18.33° K) near the end of tank expulsion, the actual NPSP being supplied is

$$\begin{aligned} \text{NPSP} &= P_t - P_{\text{GHV}} = 21 \text{ psia} - 7.9 \text{ psia} = 13.1 \text{ psia} \\ &= 145 \times 10^3 \text{ N/m}^2 - 54 \times 10^3 \text{ N/m}^2 = 91 \times 10^3 \text{ N/m}^2 \end{aligned}$$

Hence, during the latter portion of the expulsion, the net positive suction pressure is much greater than would be required. A savings of helium pressurant could be realized by varying the tank pressure to maintain a constant NPSP.

The analytical program was modified in order to compute the helium pressurant requirements for a constant NPSP. The basic mechanics of the computation remained the same, with the output parameter of primary concern again the ratio of pounds of liquid hydrogen expelled per pound of helium pressurant required.

Hot-Gas Pressurant Requirements

A theoretical analysis (ref. 5) was used to predict the weight of helium pressurant required for a hot-gas pressurization system in which the helium gas is injected through an overhead injector at 300° and 520° R (167° and 289° K). A theoretical approach was necessary since no experimental data on pressurant requirements for low tank pressure and for a flight-weight tank are available. The experimental values of tank pressure and expulsion time, along with the physical dimensions of the test tank were retained. However, the test tank wall thickness was reduced from 0.188 to 0.040 inch (0.478 to 0.102 cm) to reduce the heat-sink capacity of the test tank wall. This reduction made the predicted helium pressurant weight more representative of a flight-weight vehicle, since the magnitude of the heat-sink capacity becomes significant only when the inlet gas temperature is raised above the propellant temperature.

TEST PROCEDURE

The auxiliary bath tank was filled with liquid hydrogen up to the top liquid-level sensor. A tank pressure of approximately 3 psi ($21 \times 10^3 \text{ N/m}^2$) above atmospheric pressure was maintained at all times by the proper setting of the back-pressure relief valve. This procedure was followed to ensure a relatively constant liquid temperature, near 37° R (20.6° K), regardless of the boiloff rate due to heat addition. The bath was filled periodically by a topping process whenever the liquid interface dropped below the second liquid-level sensor.

The test tank was filled with liquid hydrogen to an arbitrary point above the top liquid-level sensor. The electric strip heaters located inside the test tank were used to

heat the propellant to the desired initial temperature. The test tank vent was back pressurized so that a vapor pressure corresponding to the desired initial liquid temperature was maintained in the ullage. The thermocouples on the vertical rake were monitored to determine when the desired temperature was reached. Once this temperature was reached, the strip heaters were turned off.

The test tank was pressurized to the desired operating level and expulsion was initiated. Visual monitoring of the top liquid-level sensors (both the hot-wire sensor and the optical sensor) indicated when the liquid interface passed this reference plane. At the instant the sensors indicated gas, a marker channel recorded with the data was manually tripped to signify the start of expulsion data. The helium flow rate during the expulsion was automatically controlled to maintain a constant tank pressure. The marker channel was again manually tripped at the instant the liquid interface passed the bottom liquid-level sensor to signify the end of the expulsion data. The actual expulsion was terminated shortly after the marker channel had been tripped.

The nominal values maintained for each of the primary test variables in the experimental program were

Tank pressure, psia (N/m^2)	21, 25, and 33 (145×10^3 , 172×10^3 , and 228×10^3)
Varying outflow rates resulting in expulsion times, sec, of -	60, 100, 200, and 300
Initial bulk liquid temperature, $^{\circ}R$ ($^{\circ}K$)	36 to 38 (20 to 21.1)

The quantity of liquid expelled during the data run varied from 9.4 to 10.4 cubic feet (0.266 to 0.294 cu m), depending on the bubble holdup volume associated with the particular tank pressure and expulsion rate being maintained. The bubble holdup volume is the volume of liquid displaced by the gas bubbles in transit from the injector to the liquid interface, and hence, it is a function of the tank pressure maintained as well as of the liquid outflow rate.

The original procedure was to fill the test tank to the exact plane of the top liquid-level sensor, pressurize, and then begin expulsion. However, the initial expulsion runs conducted showed severe transients in the flowmeter output and the orifice gas-pressure differential upon initiation of outflow. The transients experienced were attributed to the low tank pressure being maintained, inadequate control-system response, and the relatively small initial ullage volume. The error associated with the numerical integrations of the data during the transients would seriously decrease the accuracy of the results.

The expulsion was initiated when the liquid interface was somewhere above the top liquid-level sensor to eliminate these transients from the recorded expulsion data. By

the time the interface dropped to the top sensor, the transients had subsided.

An additional factor in changing the procedure was the difficulty in setting the liquid level exactly at the plane of the top sensor. A small change in pressure and/or propellant temperature would shift the interface. More repeatability with respect to initial and final liquid-level positions could be obtained by initiating expulsion before the liquid interface passed the top sensors.

Unfortunately, when the expulsion was conducted in this manner, the initial ullage volume at the initiation of outflow could not be determined exactly, since the liquid level was arbitrarily set. Therefore, a clear indication of the system performance during the pressurization and hold periods prior to expulsion could not be obtained. However, even if the initial ullage volume were known exactly, the errors in the data due to the previously mentioned transients would make the results questionable.

DATA REDUCTION

Comparison of Experimental with Ideal Helium Pressurant Requirements

As discussed previously, the bulk liquid-hydrogen temperature decreases with time during any given expulsion. The expulsion was divided into four segments to determine more fully what effect this changing temperature had on the degree of saturation of the ullage gas with hydrogen vapor. Each segment of approximately 2.5 cubic feet (0.071 cu m) represented one-fourth of the expelled liquid volume.

The position of the liquid interface with time was determined by reference to the three point sensors in the test tank and the integrated volume of liquid expelled. The height of liquid in the test tank as a function of time then established which temperature sensors were submerged in liquid at any given time. All the temperature sensors in the liquid were equally weighted to obtain an average liquid temperature at discrete times during the expulsion. The average of these temperatures over the time interval considered was then taken as representative of an average bulk liquid temperature during the expulsion of a particular segment. The theoretical ideal ratio of W_{LHX}/W_{GHe} corresponding to the computed temperature and the average tank pressure during the expulsion was then obtained from the analysis.

The experimental weight of helium pressurant required during any portion of the expulsion was determined by numerical integration of the gas orifice equation:

$$\Delta W_{GHe} = \int_{t_1}^{t_2} 0.525 Y d^2 C \sqrt{\rho_{GHe} \Delta P_o} dt$$

Similarly, the volume of liquid hydrogen expelled was determined by numerical integration of the mass flowmeter output with the following equation:

$$\Delta V_{LHX} = \int_{t_1}^{t_2} \frac{f \times FMC}{K} dt$$

The corresponding weight of liquid hydrogen expelled was obtained by multiplying the volume elements given in the preceding equation by the corresponding density of the liquid hydrogen:

$$\Delta W_{LHX} = \sum_1^n \Delta V_{LHX} \rho_{LH}$$

The density was obtained by a program subroutine which used the tank pressure and the liquid temperature measured immediately downstream of the flowmeter.

The theoretically ideal helium pressurant requirement for a measured weight of liquid hydrogen expelled can then be obtained with the following expression:

$$W_{GHe, id} = \frac{(W_{LHX})_{exp}}{\left(\frac{W_{LHX}}{W_{GHe}} \right)_{id}}$$

A descriptive measure of the effectiveness of the submerged injection technique is the percentage deviation between the experimental and ideal values of helium pressurant requirements:

$$\eta = \frac{W_{GHe, exp} - W_{GHe, id}}{W_{GHe, id}}$$

The values of η were computed for each segment. The average effectiveness over the entire run η_{av} was determined by a summation of the quantities for the four segments comprising a given expulsion.

$$\eta_{av} = \frac{\sum W_{GHe, exp} - \sum W_{GHe, id}}{\sum W_{GHe, id}}$$

$$\sum W_{GHe, exp} = \sum_{4 \text{ segments}} W_{GHe, exp}$$

$$\sum W_{GHe, id} = \sum_{4 \text{ segments}} W_{GHe, id}$$

Ullage Gas Saturation

The percentage saturation of the ullage gas with hydrogen vapor can be expressed as the ratio of the experimentally determined partial pressure of hydrogen in the ullage to the thermodynamic maximum partial pressure that could exist at the particular temperature being considered:

$$\epsilon = \frac{P_{GH, exp}}{P_{GHV}} = \frac{P_t - P_{GHe, exp}}{P_{GHV}}$$

The helium and hydrogen vapor existing in the ullage at the end of the expulsion are assumed to behave like perfect gases in the respect that

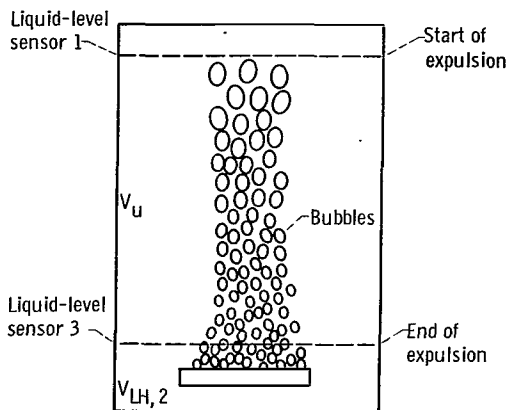
$$P_t = P_{GH} + P_{GHe}$$

The partial pressure of helium existing in the ullage at the end of the expulsion can be determined by the following equation:

$$P_{GHe} = \frac{zW_{GHe} R_{GHe} T_u}{V_u}$$

The ullage gas temperature was determined by averaging the thermocouple measurements in the gas phase over the last few seconds of the expulsion. This average temperature, in addition to being used in the preceding equation, determined the thermodynamic maximum or ideal partial pressure that could exist in the ullage.

The volume V_u that the ullage gas occupied at the end of expulsion is that volume between liquid-level sensors 1 and 3 that the liquid occupied at the start of expulsion.



The volume V_u is then the physical tank volume between sensors 1 and 3 minus the initial volume occupied by the bubbles in transit from the injector to the ullage. The following equations with the accompanying sketch indicate how a mass balance on the liquid hydrogen was performed to calculate V_u . (Subscript 1 denotes the start and subscript 2 denotes the end of expulsion.)

The weight of liquid hydrogen in the tank at the start of expulsion is equal to that at the end of expulsion plus the weights of hydrogen expelled and vaporized.

$$W_{LH, 1} = W_{LH, 2} + \Delta W_{LHX, 1-2} + \Delta W_{LHV, 1-2}$$

Data reduction yields average liquid temperatures at the start and end of expulsion as well as an average liquid temperature during the expulsion so that initial and final liquid densities as well as an average saturated vapor density can be calculated. The data also yield the weight and volume of hydrogen expelled. The volume $V_{LH, 2}$ is obtained by test-tank calibration tests and neglects the volume occupied by the bubbles between the injector and the interface at the end of expulsion. Substitution of these terms into the preceding equation yields

$$\rho_{LH, 1}(V_u + V_{LH, 2}) = \rho_{LH, 2}V_{LH, 2} + \Delta W_{LHX, 1-2} + \Delta V_{LHX, 1-2}\rho_{GHV}$$

Rearranging terms yields the final form:

$$V_u = \frac{V_{LH, 2}(\rho_{LH, 2} - \rho_{LH, 1}) + \Delta W_{LHX, 1-2} + \Delta V_{LHX, 1-2}\rho_{GHV}}{\rho_{LH, 1}}$$

RESULTS AND DISCUSSION

Comparison of Experimental with Ideal Helium Pressurant Requirements

A comparison of the experimental with the theoretical ideal helium pressurant requirement for each expulsion run conducted is tabulated in table I. The percentage increase of the experimental value over the ideal η for each of the four segments comprising a given expulsion is listed separately. For the entire run η_{av} is the percentage

deviation between the respective total values of the four segments.

As indicated in table I, the experimental value of the helium pressurant required for the expulsion of the first quarter segment varied from -2 to 44 percent greater than the theoretical ideal. The large and varying increase cannot be attributed to incomplete saturation of the helium bubbles with hydrogen vapor, but rather it is a direct result of the inherent slow response of the helium flow system together with the particular composition of the ullage gas prior to outflow. A detailed discussion of how these factors cause the discrepancy to occur is given in appendix D. However, for approximately a third of the runs listed, the experimental and the ideal helium pressurant requirements agree within 5 percent. The average deviation for the first segment for all of the runs considered showed the experimental value to be 12.8 percent greater than the ideal.

The experimental values of the weight of helium pressurant required for the expulsion of the second, third, and fourth quarter segments were in very close agreement with the computed theoretical ideal. In many cases, the experimental value for a given segment was actually less than the ideal. This result can be attributed to very small errors in computing the average experimental temperatures on which the ideal was based.

Table I shows that the percentage increase of the experimental helium pressurant weight over the ideal for the entire run η_{av} varied from -5.8 to 11.7 percent. The average percentage increase for all of the expulsion runs was 1.4 percent.

The results shown in table I indicate that the ullage gas approached 100 percent saturation (i. e., the maximum amount of hydrogen vapor thermodynamically possible existed in the ullage) independent of the tank pressure, expulsion time, or liquid temperature being maintained or measured. This conclusion can be validated in a separate manner by computing the ratio of the experimentally determined partial pressure of hydrogen in the ullage at the end of a given expulsion to the maximum that is thermodynamically stable for the particular average ullage gas temperature computed. The range of values for this saturation ratio ϵ as listed in table I is 95 to 102 percent, 96 to 106 percent, and 96 to 107 percent for tank pressures of 21, 25, and 33 psia (145×10^3 , 172×10^3 , and 228×10^3 N/m²) respectively.

The close agreement between the percentage saturation of the ullage gas ϵ and the percentage deviation between the experimental and ideal helium requirements η_{av} is to be expected, since both parameters, ϵ and η measure the degree to which the helium pressurant requirements have been minimized. (Ideally, $\eta_{av} = 0$ is equivalent to $\epsilon = 100$ percent.) The objective of evaluating both is to substantiate the results of the comparisons of ideal to experimental by basing the comparisons on representative temperatures that were computed by independent methods. The close agreement between the average liquid-hydrogen temperature $T_{LH,av}$ and the average ullage gas temperature T_u (table I) lends credence to the validity of the temperatures. Ideally, the two temperatures should be equal, since the ullage gas bubbled up through the liquid must assume the liquid temperature.

Effect of Physical Test Variables on Absolute Helium Pressurant Requirements

The average value of tank pressure during an expulsion, the measured expulsion time, and the measured average liquid temperature for a given expulsion segment are tabulated with the run data in table I. In the following comparisons, two of the parameters were held constant, while the experimental and ideal pounds of helium pressurant required as a function of the pounds of liquid hydrogen expelled were plotted. Each data run considers the four segments comprising a given expulsion; hence, four accumulative values appear in each of the figures 4 to 6.

The effect of three different average liquid-hydrogen temperatures on the helium pressurant requirements when the tank pressure was held constant at 25 psia ($172 \times 10^3 \text{ N/m}^2$) and the expulsion time was held constant at 60 seconds is shown in figure 4. The experimental values of helium pressurant required are almost identical to the predicted ideal for each of the three average liquid temperatures considered. In addition, the weight of helium required to expel a given weight of liquid hydrogen decreases with increasing temperature because the higher vapor pressure which may be used at the higher temperature reduces the required partial pressure of helium.

The effect of three different tank pressures on the helium pressurant requirements when the expulsion time was held constant at 300 seconds and the average liquid-hydrogen temperature held constant at 37.2° R (20.7° K) is shown in figure 5. Again the experimental values of helium pressurant requirements are very near the predicted ideal for each of the three tank pressures considered. The deviations between experimental and ideal in runs 10 and 21 occur in the first expulsion segment. Since the plotted values are accumulative, the same deviation is carried into the fourth expulsion segment. The weight of helium pressurant increases sharply with increasing tank pressure, since a higher partial pressure of helium must be provided to the constant partial pressure of hydrogen vapor being supplied.

Figure 6 compares run 6 with run 10, for which tank pressure was constant at 21 psia ($145 \times 10^3 \text{ N/m}^2$), and run 15 with run 21, for which tank pressure was constant at 25 psia ($172 \times 10^3 \text{ N/m}^2$). All runs were made at an average liquid temperature of 36° R (20° K). The change in expulsion time from 100 to 300 seconds had no effect on the experimental helium pressurant requirements in either case, which indicates that the process is not time dependent. Again, an increased tank pressure increased the helium pressurant requirements, as shown previously.

The maximum or ideal weight of hydrogen that can be vaporized during any given expulsion is a direct function of the average liquid temperature during the expulsion, since this temperature determines the maximum vapor pressure of hydrogen that can exist in the ullage. The weight of hydrogen vaporized must be independent of the tank pressure level being held for a given average liquid temperature. The quantity of hydro-

gen vaporized during any of the expulsions is then independent of the weight of helium bubbled up through the hydrogen. Because of the complexity of the process and a lack of visual observation of the injection of the helium bubbles into the liquid, a correlation between total tank pressure and surface area of injected helium bubbles could not be obtained. In general, a higher partial pressure of helium in the ullage would ensure a higher surface area for evaporation and diffusion to occur.

Further proof that the amount of hydrogen vaporized is independent of the weight of helium bubbled through the liquid can be shown by comparing temperature profiles for the complete expulsion. Figure 7 shows the four average temperatures for runs 9, 20, and 29 for which the corresponding tank pressures were 21, 25, and 33 psia (145×10^3 , 172×10^3 , and 228×10^3 N/m²). The average temperatures are essentially the same throughout the expulsion. Since the degree of cooling of the propellant is directly proportional to the weight of hydrogen vaporized, the amount of hydrogen vaporized in each case must be the same.

The degree of saturation measured for the fourth expulsion segment approached the thermodynamic limit. Since the column of liquid above the injector was constantly decreasing, it can be concluded that a varying liquid height had no effect on the performance of the injection technique. Therefore, the major portion of hydrogen evaporated and diffused into the helium bubbles occurred immediately upon injection of the bubbles into the liquid.

The effect of a varying propellant temperature on the ratio of the weight of liquid hydrogen expelled per pound of helium pressurant required is illustrated in figure 8 for the three tank pressures used. The experimentally determined ratio was plotted for each of the expulsion segments, and a solid line was faired through the experimental points.

As shown in figure 8 the preceding ratio decreases markedly with decreasing temperature for any given tank pressure. As the temperature of the liquid decreases, a higher partial pressure of helium must exist in the ullage to compensate for the decreased partial pressure of hydrogen which results from the lower saturated vapor pressure of the liquid.

Heating the helium pressurant would serve to maintain a more constant liquid temperature and thus a constant partial pressure of hydrogen in the ullage throughout the expulsion. Introducing more heat with the helium pressurant than would be removed by the evaporation process, however, would increase the potential partial pressure of hydrogen in the ullage and by so doing would increase the total tank pressure required if the partial pressure of helium were to be maintained constant.

The relative change in the ratio W_{LHX}/W_{GHe} becomes more pronounced as the total tank pressure is decreased. This condition is caused by the relative change in the minimum partial pressure requirements of helium as shown in the following table:

Average liquid-hydrogen temperature, $T_{LH,av}$		Weight of liquid-hydrogen expelled per unit weight of gaseous helium required, W_{LHX}/W_{GHe}	Saturated hydrogen vapor pressure, P_{GHV}		Tank pressure, P_t		Gaseous helium pressure, P_{GHe}	
$^{\circ}R$	$^{\circ}K$		psia	N/m^2	psia	N/m^2	psia	N/m^2
37.0	20.6	87.5	16.0	110×10^3	21.0	145×10^3	5.0	35×10^3
34.0	18.9	36.0	9.5	66	21.0	145	11.5	79
37.0	20.6	24.8	16.0	110	33.0	228	17.0	117
34.0	18.9	17.3	9.5	66	33.0	228	23.5	162

At any given liquid temperature, the weight of helium pressurant required to expel 1 pound (0.95 kg) of liquid hydrogen is directly proportional to the partial pressure of helium being supplied. The following table illustrates this requirement for a constant liquid temperature of $36^{\circ}R$ ($20^{\circ}K$) for which the saturated vapor pressure is 13.6 psia ($93.8 \times 10^3 N/m^2$).

Tank pressure, P_t		Gaseous helium pressure, P_{GHe}		Weight of liquid hydrogen expelled per unit weight of gaseous helium required, W_{LHX}/W_{GHe}	Weight of gaseous helium required to expel a unit weight of liquid hydrogen, W_{GHe}/W_{LHX}	Weight of gaseous helium required to expel a unit weight of liquid hydrogen per unit of partial pressure of helium supplied, $(W_{GHe}/W_{LH,2})/P_{GHe}$
psia	N/m^2	psia	N/m^2			
20.9	144×10^3	7.3	50×10^3	56.6	0.0177	0.0024
24.9	172	11.3	78	36.6	.0273	.0024
32.9	227	19.3	133	21.5	.0465	.0024

The probable error in the reading of any given temperature sensor was calculated to be $\pm 0.27^{\circ}R$ ($\pm 0.15^{\circ}K$). The dashed curves in figure 8 indicate the boundaries of the ratio W_{LHX}/W_{GHe} , if the limits of the error exist. The band of error increases with increasing temperature, again because of the variance of saturated vapor pressure with temperature. The experimental data points represented by the solid curves all fall within the theoretical band imposed, except for high temperatures. This condition is, of course, caused by the previously described phenomena that occur in the first expulsion segment.

Heat-Transfer Effects

The results of table 1 show that the computed effectiveness of the submerged injector increased during the expulsion. The average percentage increase of the experimental over the ideal for all runs conducted was 12.8, 0.9, 0.4, and -1.8 percent for the first, second, third, and fourth expulsion segments, respectively. Since the increase occurring in the first segment has already been discussed, this section emphasizes the second, third, and fourth expulsion segments and, in particular, why the experimental weight of helium pressurant used in the fourth expulsion segment was less than the ideal.

Since the liquid temperature in the test tank was decreasing during any given expulsion, a driving potential for heat transfer by conduction between the test tank and the bath tank at a constant temperature (37°R (20.6°K)) was established. If it is assumed that the polyester film on the exterior surface of the cork insulation is an effective vapor barrier, the heat leak from the bath tank into the test tank could approach a maximum of 0.9 Btu (950 J) for any expulsion. The potential heat capacity of the test tank wall, in going from an initial temperature of 37°R (20.6°K) to a final temperature of 34°R (18.9°K) at the end of expulsion, could approach 0.8 Btu (840 J). The heat conduction and potential heat capacity of the wall could then conceivably contribute a maximum of 1.7 Btu (1790 J) into the test tank during any given expulsion. Based on a heat of vaporization of liquid hydrogen of 194 Btu per pound (451×10^3 J/kg), this 1.7 Btu (1790 J) could vaporize an insignificant 0.009 pound (0.004 kg) of liquid.

A more significant argument to justify specifically the performance during the fourth expulsion segment results from the radial temperature gradients encountered in using a finite area for the submerged injector. The radial temperature profiles for run 28 in which tank pressure was 33 psia (228×10^3 N/m²) and expulsion time was 207 seconds are shown in figure 9(a). The plane 1 inch (2.5 cm) above the injector is represented by temperature sensors 12 to 14 and 16, as previously shown in figure 2. Throughout the expulsion, these sensors are continuously submerged in liquid. The profile is essentially flat except for the sharp dropoff in the immediate vicinity of the injector. The severity of the dropoff does not appear to change with time. A nearly constant value of 1.5°R (0.83°K) exists between sensors 12 to 14 and sensor 16, regardless of which expulsion segment is considered. For a short portion of the test program, temperature sensors 1 and 15 were removed from the original configuration as shown in figure 2 and placed on a horizontal arm in the plane of sensor 7 (24.7 in. (62.7 cm) above the injector). The profile obtained in this plane (fig. 9(b)), is also flat regardless of whether it is in the liquid or gas phase. The average temperature of the liquid is essentially the same in each plane for the first two expulsion segments, which proves that no vertical temperature gradients exist. During the third and fourth expulsion segments, the sensors in the plane 24.7 inches (62.7 cm) above the injector are in the gas phase. As shown, the gas temperature does not change with time.




Figure 9(b) illustrates the radial temperature profiles for run 24, in which the tank pressure was again 33 psia ($228 \times 10^3 \text{ N/m}^2$), but the expulsion time was 59 seconds. The profile for each expulsion segment is again essentially flat except that the dropoff in the immediate vicinity of the injector now approaches 3° R (1.7° K). This dropoff occurs because less time is available to transfer heat from the warmer liquid to the colder liquid in the vicinity of the injector.

The limited area injector then established a region of lower liquid temperature into which the helium gas was injected. Since all the liquid temperature measurements were equally weighted, the experimentally determined average bulk liquid-hydrogen temperature against time was less than the theoretical ideal which removes heat uniformly from the bulk liquid. As shown in figure 10 for run 24, the discrepancy increases as the expulsion continues and reaches a maximum at the end of expulsion.

Therefore, a region of warmer liquid existed near the test tank wall during the expulsion of the fourth segment. Hydrogen could vaporize from the surface of this warmer liquid, since the partial pressure being established by the hydrogen vapor carried to the ullage by the injected helium would be less than the saturated vapor pressure of the warmer liquid. The net result is that hydrogen vapor was supplied to the ullage over and above that vapor contributed by the injection technique.

Regardless of any heat-transfer effects, the important consideration in this study was to be certain that the calculated system performance was based on representative temperatures. This was shown previously by noting the very close agreement between the average ullage gas temperature at the end of a given run and the average bulk liquid temperature measured during that run. Further substantiation of this agreement can be noted by comparing the changing average bulk liquid-hydrogen temperature with the average ullage gas temperature at the end of expulsion (fig. 10). The average ullage gas temperature at any vertical position in the tank must represent the average bulk liquid temperature when the interface passed this point during the expulsion. As shown in figure 10, the two profiles are extremely close together.

The preceding discussion has indicated a distinct disadvantage of limited area injectors. If the injector area were, in the extreme case, simply the cross-sectional area of the pressurant supply line, severe subcooling of the propellant would result. The injected helium bubbles would saturate with hydrogen vapor at a pressure corresponding to this low temperature. However, once the bubbles are injected, bubble coalescence occurs and bubble size increases. Hence, subsequent passage of the bubbles into warmer liquid where a higher vapor pressure is available may not necessarily mean that the individual bubbles will again become saturated. In other words, the surface-area to volume ratio of the bubble may have decreased to the point where additional mass transfer of hydrogen vapor into the bubbles is impeded. The net effect would be the inability to saturate the individual bubbles to the thermodynamic limit. Whether or not

sufficient hydrogen would be vaporized from the interface to supplement the vapor entrained in the bubbles is questionable.

The optimum concept would be to inject the helium pressurant into the liquid uniformly over the entire cross-sectional area of the tank. The plane of the injector would be as near the outlet as possible to maximize the amount of liquid through which the helium is bubbled at any time, as well as to minimize the residual liquid at the end of expulsion. However, the restriction that no bubbles be carried out with the expelled liquid must be considered.

Analytical Comparison of Pressurant Weights of Submerged Injection with Overhead Injection

Since evaluation of the experimental results indicated that the ullage gas was nearly 100 percent saturated with hydrogen vapor, the theoretical analysis was used to calculate the helium pressurant requirements for the submerged injector. An initial bulk liquid-hydrogen temperature of 37.35°R (20.75°K), corresponding to a saturated vapor pressure of 17 psia ($117 \times 10^3 \text{ N/m}^2$), was used for both conditions, tank pressure held constant and net positive suction pressure NPSP held constant. The tank pressures of 19, 21, 25, and 33 psia (131×10^3 , 145×10^3 , 172×10^3 , and $228 \times 10^3 \text{ N/m}^2$) selected represented initial NPSP of 2, 4, 8, and 16 psia (14×10^3 , 28×10^3 , 55×10^3 , and $110 \times 10^3 \text{ N/m}^2$) respectively. Complete ullage gas saturation for a tank pressure of 19 psia ($131 \times 10^3 \text{ N/m}^2$) and/or a varying tank pressure (NPSP held constant) was not verified in the experimental program. However, the overall program results would seem to indicate that no significant change from 100 percent saturation should be anticipated.

Comparisons of the helium pressurant requirements for the submerged injector to those analytically predicted for a hot-gas overhead injector utilizing inlet gas temperatures of 300° and 520°R (167° and 289°K) are shown in figure 11. In general, the comparisons show the submerged injector pressurant requirements to be very competitive, with respect to weight, for low values of NPSP. At 19 psia ($131 \times 10^3 \text{ N/m}^2$) (fig. 11(a)), the submerged injector matches the overhead injector for a constant pressure and is better by a factor of 2 when the NPSP is maintained constant. At 21 psia ($145 \times 10^3 \text{ N/m}^2$) (fig. 11(b)), the pressurant weight requirement for the submerged injector is $1\frac{1}{2}$ times greater when tank pressure is held constant but it is slightly less than that for the overhead injector when the NPSP is maintained constant. At 25 psia ($172 \times 10^3 \text{ N/m}^2$) (fig. 11(c)), the submerged injector pressurant weight is $1\frac{1}{2}$ times greater for a constant NPSP. At 33 psia ($228 \times 10^3 \text{ N/m}^2$) (fig. 11(d)), the submerged injector is nowhere near competitive with the overhead injector.

The helium pressurant weight savings that may be realized by controlling the pres-

surant flow to maintain a constant NPSP rather than a constant tank pressure are clearly evident. In a flight vehicle, the NPSP could be maintained relatively constant simply by regulating the helium volume flow rate to be proportional to the liquid volume outflow rate. An alternative method would involve sensing the propellant temperature at the pump inlet and then programing a varying tank pressure to be maintained.

Thus far, only the helium pressurant weight required for expulsion has been considered. However, the weight of vaporized propellant must also be taken into account. The total pressurant gas weights required for expulsion are shown in figure 12. Tank pressures of 19, 21, and 25 psia (131×10^3 , 145×10^3 , and 172×10^3 N/m²) are considered for both cases in which the tank pressure is held constant and when the NPSP is held constant. As shown in figure 12, the amount of hydrogen vaporized is independent both of the tank pressure maintained and of the controlling feature used. The weight of hydrogen vaporized was 0.82 pound (0.37 kg) for 45.6 pounds (20.7 kg) of liquid hydrogen expelled, which was 1.8 percent of the original weight of liquid hydrogen. The important aspect is, however, the fact that a portion of the pressurant can be stored much more effectively (less overall weight) as a liquid than as a gas.

CONCLUSIONS

The helium pressurant requirements for a submerged injector are competitive with a hot-gas overhead injector only for low net positive suction pressures NPSP ranging from 0 to 4 psi (28×10^3 N/m²). Since the NPSP being maintained is the partial pressure of helium being supplied, the ratio of the pounds of liquid hydrogen expelled per pound of helium pressurant required is directly proportional to the NPSP.

Significant helium pressurant savings with the submerged injector can be realized if the test tank pressure can be varied during the expulsion so that a constant NPSP is maintained. For a NPSP of 2 psia (14×10^3 N/m²) (initial tank pressure, 19 psia (131×10^3 N/m²)), the helium pressurant required for the submerged injector is less than one-half that required for the hot-gas overhead injector utilizing an inlet gas temperature of 520° R (289° K).

Further evaluation of the experimental data showed the following results:

1. The ullage gas was essentially 100 percent saturated with hydrogen vapor at any time during a given expulsion, (i. e., the partial pressure of hydrogen vapor in the ullage was equal to the saturated vapor pressure at the particular temperature considered).
2. The degree of ullage gas saturation obtained was not dependent on the tank pressure maintained, the measured expulsion time, or the average bulk liquid-hydrogen temperature at any time during a given expulsion.

3. The major portion of the evaporation and diffusion of hydrogen into the helium bubbles occurred immediately upon injection of the helium into the liquid.

4. The agitation of the liquid combined with the heat removal capability of the bubbles as the bubbles pass through the interface eliminates any thermal gradients in the vertical plane.

5. The hydrogen vaporized constitutes an additional weight not found in the hot-gas system. However, storage of this vapor as a liquid minimizes the overall weight penalty.

Lewis Research Center,
National Aeronautics and Space Administration,
Cleveland, Ohio, March 22, 1967,
180-31-02-01-22.

APPENDIX A

SYMBOLS

C	orifice coefficient of discharge	Y	orifice plate expansion factor
c	specific heat, Btu/(lb)(^o R) (J/(kg)(^o K))	z	compressibility factor for gas
d	diameter, in. (cm)	ε	saturation, percent
FMC	flowmeter calibration, cps/count	η	percentage increase of experimental over ideal
f	flowmeter output, cps	ρ	density, lb/ft ³ (kg/m ³)
ΔH	heat of vaporization, Btu/lb (J/kg)	Subscripts:	
K	flowmeter constant, cycles/ft ³ (cycles/m ³)	av	average
NPSP	net positive suction pressure, psia (N/m ²)	c	thermal contraction
P	pressure, psia (N/m ²)	exp	experimental
ΔP	differential pressure, psi (N/m ²)	GH	gaseous hydrogen
ΔQ	incremental heat, Btu (J)	GHe	gaseous helium
R	gas constant, ft/ ^o R (m/ ^o K)	GHV	saturated hydrogen vapor
T	temperature, ^o R (^o K)	id	ideal
ΔT	incremental temperature, ^o R	LH	liquid hydrogen
t	time, sec	LHV	liquid hydrogen vaporized
V	volume, ft ³ (m ³)	LHX	liquid hydrogen expelled
\dot{V}	volume flow rate, ft ³ /sec (m ³ /sec)	o	orifice
ΔV	incremental volume, ft ³ (m ³)	t	tank
W	weight, lb (kg)	u	ullage
\dot{W}	weight flow rate, lb/sec (kg/sec)	1	start of expulsion
ΔW	incremental weight, lb (kg)	2	end of expulsion
		1-2	time from start to end of expulsion

APPENDIX B

INJECTOR FACE MATERIAL SELECTION AND PRELIMINARY TESTING

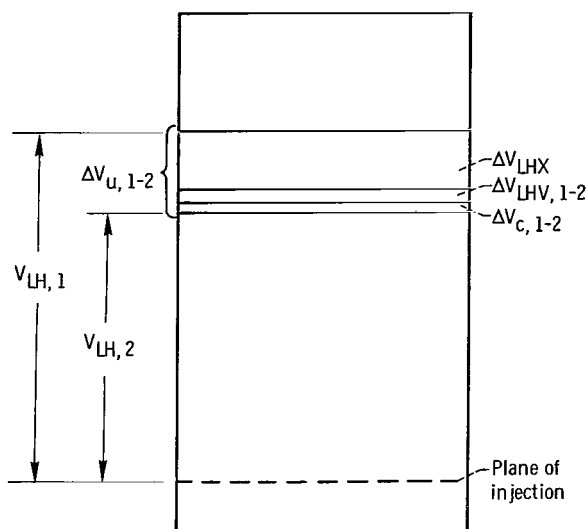
The selection of the submerged injector face material was oriented toward increasing the probability of completely saturating the individual helium bubble immediately upon injection into the liquid. The time required to approach phase equilibrium (i. e. , the partial pressure of hydrogen vapor in the bubble equal to the saturated vapor pressure of the liquid) can be minimized by maximizing the surface area to volume ratio of the injected bubble. Since the evaporation process removes heat from the bulk liquid, the maximum amount of dispersion of the injected bubbles would eliminate severe localized subcooling of the propellant. With the above dispersion and a minimum bubble size and injection velocity, a high degree of saturation can be anticipated before bubble coalescence becomes a major factor in decreasing the surface-area to volume ratio of the individual bubble.

A porous metal material with low permeability and with individual pore openings in the micron range can be obtained by a flat plate composed of multilayer screens sintered together. The material selected for the injector has a nominal micron rating of less than 5, which was the tightest weave practical to manufacture and still control the uniformity. Furthermore, at any lower permeability, the material will plug easily in the presence of any contamination. The aforementioned permeability established the maximum injector face area possible to ensure a uniform flow distribution over the entire injector area for the predicted low helium pressurant flow rates. The maximum area was obtained with an injector diameter of 12 inches (30.5 cm).

The injector was tested for uniformity of flow and pressure drop by simulating the predicted pressurant volume flow with gaseous helium bubbled through water. Figure 13 shows a side view of the uniformity of the bubble pattern observed. A smaller injector with the same face material was tested in a portable liquid-hydrogen facility using helium pressurant bubbled through liquid hydrogen. A visual observation of the flow pattern confirmed the suitability of the injector face material.

APPENDIX C

THEORETICAL ANALYSIS USED TO COMPUTE IDEAL HELIUM PRESSURANT REQUIREMENTS FOR GIVEN EXPULSION SEGMENT



The following equations and the accompanying sketch illustrate the computations for the expulsion of any given liquid volume increment ΔV_{LHX} . Subscript 1 refers to the start, and subscript 2 refers to the end of the expulsion of a typical segment. The density, specific heat, and heat of vaporization terms in the following expressions were obtained with curve fits of the appropriate property data in terms of temperature and/or pressure. The subscripts 1 and 2 then denote at what temperature and/or pressure the property was evaluated.

The weight of liquid hydrogen above the plane of the injector at the start is the density of the liquid times the volume the liquid occupies:

$$W_{LH,1} = \rho_{LH,1} V_{LH,1}$$

The weight of liquid hydrogen expelled is the density times the volume of the increment considered:

$$\Delta W_{LHX,1-2} = \rho_{LH,1} \Delta V_{LHX}$$

The weight of hydrogen vaporized can be approximated by the saturated vapor density times the volume increment:

$$\Delta W_{LHV, 1-2} = \rho_{GHV, 1} \Delta V_{LHX}$$

The quantity of heat removed from the bulk liquid is the quantity of hydrogen vaporized times the heat of vaporization:

$$\Delta Q_{1-2} = \Delta W_{LHV, 1-2} \Delta H_1$$

The change in the average bulk liquid temperature is the heat removed divided by the product of the total weight of liquid hydrogen times the specific heat:

$$\Delta T_{1-2} = \frac{\Delta Q_{1-2}}{W_{LH, 1} C_{LH, 1}}$$

The new bulk liquid-hydrogen temperature after the expulsion of the segment is then given by

$$T_{LH, 2} = T_{LH, 1} - \Delta T_{1-2}$$

The volume occupied by the remaining liquid is the initial weight of liquid minus the quantity expelled and vaporized divided by the new density:

$$V_{LH, 2} = \frac{W_{LH, 1} - \Delta W_{LHX, 1-2} - \Delta W_{LHV, 1-2}}{\rho_{LH, 2}}$$

The ullage volume created by the expulsion of the liquid segment is the difference between the initial and final volumes occupied by the liquid:

$$\Delta V_{u, 1-2} = V_{LH, 1} - V_{LH, 2}$$

The maximum partial pressure of hydrogen that can exist in this ullage volume segment is the saturated vapor pressure of the bulk liquid at the initial temperature:

$$P_{GHV, 1} = f(T_{LH, 1})$$

The partial pressure of helium that must be supplied is then the difference between the tank pressure and the saturated vapor pressure:

$$P_{\text{GHe}, 1-2} = P_t - P_{\text{GHV}, 1}$$

and the weight of helium that must be supplied is

$$\Delta W_{\text{GHe}, 1-2} = (\rho_{\text{GHe}, 1})(\Delta V_{u, 1-2})$$

APPENDIX D

ANALYSIS OF FIRST EXPULSION SEGMENT

Figure 14 depicts the tank pressure, liquid-hydrogen outflow rate, and helium pressurant flow rate as functions of time for a typical data run. Point A represents the end of the ramp-hold period and the initiation of liquid outflow. Immediately upon outflow, a drop in tank pressure to point B resulted from a ullage volume increase with no addition of pressurant gas. Not until point C was reached did the helium pressurant flow rate become sufficiently large to start the tank pressure recovery back up to the nominal operating level. At point D, the tank pressure recovery was complete. The inherent slow response of the gas flow system demonstrated from points A to B is shown again by permitting the tank pressure to exceed the desired control pressure at point D.

The obvious increase in helium pressurant flow rate above the predicted ideal from point C resulted from the fact that some liquid was expelled before a significant helium pressurant flow rate was established. However, this deficit would be overcome once the tank pressure had recovered. If point D occurred prior to the start of the first segment of data expulsion, no increase in helium requirements during the first segment could be attributed to this. Since it was not possible to set the initial liquid level at the same plane for all the data runs, some of the runs did show point D occurring after the start of the first expulsion segment.

As the expulsion continued from point D, the actual helium pressurant flow rate did not drop immediately to the predicted ideal. The following discussion indicates why this discrepancy occurred as a function of a changing ullage gas composition dictated by a fluctuating ullage gas temperature.

Unfortunately, no temperature probes were located in the ullage gas to validate any temperature fluctuations for the data runs evaluated. However, preliminary checkout runs were made with the initial liquid level near the center of the test tank, and thus several temperature probes were exposed to the ullage gas. Figure 15 shows tank pressure, liquid outflow rate, helium pressurant flow rate, and average ullage gas temperature together with average liquid temperature for a typical run. The liquid temperature was slightly higher than the ullage gas temperature at the start of helium flow because of surges in ullage gas venting that occurred while the electric strip heaters were increasing the propellant temperature. This temperature discrepancy is thermodynamically possible as long as the temperature of the liquid at the interface is equal to the ullage gas temperature. During the ramp period (pressurization to the operating level with no outflow), the addition of helium to the ullage increased the ullage gas temperature. This result was thermodynamically feasible since the addition of mass into a control volume does work on the gas initially present. The addition of energy to the control volume results in a temperature rise.

The helium pressurant added during the ramp period is, furthermore, entraining hydrogen in the bubbles and carrying it into the ullage. If the ullage gas temperature did not increase, this hydrogen would condense back to liquid, for it would not be thermodynamically stable. However, since the temperature is increasing, a higher partial pressure of hydrogen can exist in the ullage than the liquid temperature would dictate. Once expulsion is initiated, the ullage gas expands and causes a temperature drop. The hydrogen vapor carried into the ullage during the ramp by the helium bubbles must start to condense out. The condensed hydrogen vapor must be replaced by pure helium pressurant to maintain the tank pressure at a set level. This added helium pressurant requirement then affects the evaluation of the data for the first expulsion segment.

The length of time required for the ullage to regain thermodynamic equilibrium (i. e. , when the experimental helium pressurant flow rate approaches the ideal) seemed to be governed by the severity of the initial transients together with the magnitudes of tank pressure and outflow rate being maintained. In some expulsion runs, an immediate surge in the helium weight flow occurred and established equilibrium conditions prior to the start of the first data segment.

For some expulsions at 21 psia ($145 \times 10^3 \text{ N/m}^2$), no prepressurization was required. The ullage gas pressure composed of pure hydrogen vapor was already equal to the desired control pressure. All attempts to reduce this pressure by venting the test tank resulted in decreasing the propellant temperature. The apparent solution would have been to let the time period between ramp and initiation of outflow become sufficiently long to permit thermal equilibrium to occur. However, by doing this, sufficient heat may have been lost by the propellant to the bath to nullify preliminary heating obtained with the electric strip heaters.

REFERENCES

1. Schmidt, A. F.: Experimental Investigation of Liquid-Hydrogen Cooling by Helium Gas Injection. Advances in Cryogenic Engineering. Vol. 8. K. D. Timmerhaus, ed., Plenum Press, 1962, pp. 521-528.
2. Larsen, P. S.; Randolph, W. O.; Vaniman, J. L.; and Clark, J. A.: Cooling of Cryogenic Liquids by Gas Injection. Advances in Cryogenic Engineering. Vol. 8. K. D. Timmerhaus, ed., Plenum Press, 1962, pp. 507-520.
3. Mann, D. M.: The Thermodynamic Properties of Helium from 3 to 300⁰ K Between 0.5 and 100 Atmospheres. Tech. Note 154, National Bureau of Standards, Jan. 1962.
4. Goodwin, R. D.; Diller, D. E.; Roder, H. M.; Younglove, B. A.; and Weber, L. A.: Provisional Thermodynamic Functions for Para-Hydrogen in Liquid, Fluid and Gaseous States at Temperatures up to 100⁰ K and at Pressures up to 340 ATM. Rep. No. 6791, National Bureau of Standards, Aug. 4, 1961.
5. Roudebush, William H.: An Analysis of the Problem of Tank Pressurization During Outflow. NASA TN D-2585, 1965.

TABLE I. - COMPARISON OF EXPERIMENTAL

(a) U. S.

Run	Ex-pulsion time, sec	Average tank pressure, P _{t, av'} psia	First segment				Second segment				Third	
			Average liquid-hydrogen temperature, T _{LH, av'} °R	Ideal incremental weight of gaseous helium, ΔW _{GHe, id'} lb	Experi-mental incremental weight of gaseous helium, ΔW _{GHe, exp'} lb	Percentage increase of experi-mental over ideal, η	Average liquid-hydrogen temperature, T _{LH, av'} °R	Ideal incremental weight of gaseous helium, ΔW _{GHe, id'} lb	Experi-mental incremental weight of gaseous helium, ΔW _{GHe, exp'} lb	Percent-age increase of experi-mental over ideal, η	Average liquid-hydrogen temperature, T _{LH, av'} °R	Ideal incremental weight of gaseous helium, ΔW _{GHe, id'} lb
1	77	21.01	37.75	0.0761	0.0934	22.7	37.19	0.1147	0.1273	11.0	36.05	0.1946
2	74	20.95	37.1	.1194	.1397	17.0	36.5	.2820	.1673	2.9	35.8	.4874
3	93	20.96	37.78	.0733	.0992	35.3	37.13	.1201	.1303	8.5	36.45	.1619
4	97	20.93	37.3	.1088	.1363	25.3	36.8	.1460	.1603	9.8	36.0	.1943
5	99	21.00	37.66	.0856	.0968	13.0	37.06	.1255	.1224	-2.5	36.15	.1826
6	102	20.95	37.04	.1271	.1475	16.1	36.49	.1676	.1576	-6.0	35.80	.2118
7	201	20.88	37.77	.0759	.1093	44.1	37.12	.1217	.1371	12.7	36.24	.1821
8	199	20.88	37.1	.1182	.1351	14.3	36.6	.1531	.1580	3.2	36.0	.2001
9	304	20.85	37.75	.0752	.0930	23.6	37.10	.1216	.1364	12.2	36.33	.1789
10	297	20.90	37.2	.1143	.1329	16.3	36.6	.1532	.1615	5.4	35.9	.2059
11	60	24.93	37.47	.1898	.2125	11.9	36.81	.2395	.2313	-3.4	35.78	.3071
12	58	24.93	36.76	.2321	.2382	2.6	36.18	.2639	.2615	-.9	35.21	.3235
13	60	24.90	36.05	.2829	.2931	3.6	35.50	.3213	.3063	-4.7	34.82	.3701
14	98	24.90	37.8	.1703	.1941	14.0	37.2	.2087	.2165	3.7	36.3	.2777
15	97	24.87	37.2	.2058	.2288	11.2	36.6	.2444	.2511	2.7	35.8	.3133
16	97	24.93	36.07	.2866	.2875	.3	35.60	.3180	.3046	-4.2	34.93	.3553
17	198	24.89	37.9	.1664	.2042	22.7	37.1	.2243	.2357	5.1	36.4	.2787
18	198	24.89	37.34	.2046	.2242	9.6	36.78	.2458	.2338	-4.9	36.02	.2952
19	198	24.86	36.28	.2810	.2765	-1.6	35.90	.3094	.2946	-4.8	35.12	.3629
20	299	24.89	37.8	.1762	.2278	29.3	37.1	.2283	.2424	6.2	36.2	.2909
21	300	24.86	37.2	.2181	.2475	13.5	36.5	.2672	.2673	0	35.8	.3196
22	300	24.93	36.10	.2981	.2965	-.5	35.72	.3286	.3088	-6.0	35.05	.3694
23	65	32.55	37.55	.4678	.5397	15.4	36.66	.4604	.4624	0.4	35.86	.4962
24	59	32.98	37.05	.3969	.3878	-2.3	36.28	.4659	.4399	-5.6	35.61	.5027
25	96	32.92	37.7	.3721	.4077	9.6	37.0	.4067	.4117	1.2	36.2	.4450
26	94	32.85	37.0	.3962	.4013	1.3	36.4	.4393	.4333	-1.4	35.7	.5276
27	203	32.92	37.87	.3734	.3805	1.9	37.21	.4313	.4043	-6.2	36.40	.4912
28	207	32.99	37.23	.4309	.4548	5.5	36.80	.4716	.4433	-6.0	36.06	.5303
29	297	32.74	37.8	.3790	.4007	5.7	37.1	.4338	.4400	1.4	36.3	.4907
30	306	32.72	37.3	.4157	.4269	2.7	36.7	.4634	.4518	-2.5	36.0	.5335

RESULTS WITH THEORETICAL IDEAL

customary units

segment		Fourth segment				Average percentage increase, η_{av}	Average liquid-hydrogen temperature for the entire expulsion, $T_{LH,av}'$ °R	Average ullage gas temperature at end of run, $T_{u,av}'$ °R	Average experimental gaseous hydrogen pressure for the entire expulsion, $P_{GH,exp}'$ psia	Average ideal gaseous hydrogen pressure for the entire expulsion, $P_{GH,id}'$ psia	Saturation, ϵ , percent
Experimental incremental weight of gaseous helium, $\Delta W_{GHe,exp}'$ lb	Percentage increase of experimental over ideal, η	Average liquid-hydrogen temperature, $T_{LH,av}'$ °R	Ideal incremental weight of gaseous helium, $\Delta W_{GHe,id}'$ lb	Experimental incremental weight of gaseous helium, $\Delta W_{GHe,exp}'$ lb	Percentage increase of experimental over ideal, η						
0.1887	-3.0	34.07	0.3161	0.3231	2.2	4.4	36.27	36.46	14.01	14.7	95.3
.2195	6.9	34.1	.7901	.3105	1.6	5.9	35.88	35.94	12.95	13.5	95.9
.1782	10.1	35.03	.2115	.2255	6.6	11.7	36.60	36.69	14.50	15.29	95.1
.2092	7.6	34.7	.2188	.2199	.5	8.7	36.2	36.27	13.73	14.20	96.7
.1677	-8.1	34.78	.2789	.2585	-7.3	-4.1	36.41	36.45	14.86	14.70	101.1
.2104	-7	34.48	.2986	.2810	-5.9	-1.1	35.95	35.88	13.61	13.30	102.3
.1980	8.7	34.67	.2810	.2846	1.3	10.4	36.45	36.35	14.12	14.40	98.1
.2133	6.6	34.4	.2961	.2905	-1.9	3.8	36.03	36.09	13.44	13.80	97.4
.1982	10.8	34.83	.2724	.2807	3.0	9.3	36.48	36.38	14.27	14.50	98.4
.2162	5.0	34.4	.3011	.2909	-3.4	3.5	36.03	36.08	13.46	13.80	97.5
.3039	-1.0	34.20	.4043	.4080	0.9	1.3	36.07	36.19	13.67	14.05	97.3
.3117	-3.6	33.78	.4463	.4384	-1.8	-1.3	35.48	35.59	12.57	12.65	99.4
.3527	-4.7	33.17	.4621	.4268	-7.6	-4.0	34.89	34.93	11.79	11.30	104.3
.2904	4.6	34.5	.3957	.3822	-3.4	2.9	36.45	36.54	14.43	14.90	96.8
.3158	.8	34.3	.4009	.4051	1.0	3.1	35.98	35.93	13.24	13.40	98.8
.3389	-4.6	33.77	.4286	.4026	-6.1	-4.0	35.09	35.01	12.21	11.50	106.2
.2937	5.4	34.7	.3931	.3874	-1.5	5.5	36.53	36.40	14.33	14.55	98.5
.2785	-5.7	34.67	.3924	.3632	-7.5	-3.4	36.20	36.26	14.46	14.20	101.8
.3371	-7.1	34.02	.4217	.3905	-7.4	-5.6	35.33	35.35	12.86	12.20	105.4
.3051	4.9	34.8	.3853	.3899	1.2	7.8	36.48	36.43	14.02	14.60	96.0
.3233	1.2	34.4	.4078	.3929	3.7	1.5	35.98	35.99	13.45	13.60	98.9
.3468	-6.1	34.01	.4316	.4420	2.4	-5.5	35.22	35.30	12.58	12.05	104.4
.5027	1.3	34.21	.5877	.5936	1.0	4.3	36.07	36.04	13.42	13.75	97.6
.4825	-4.0	34.00	.6120	.5886	-3.8	-4.0	35.74	35.86	13.80	13.25	104.2
.4515	1.5	34.5	.6667	.6659	-.1	2.4	36.35	36.36	13.92	14.40	96.7
.5266	-.2	34.0	.6376	.6241	-2.1	-.8	35.78	35.90	13.18	13.35	98.7
.4563	-7.1	35.17	.5844	.5308	-9.2	-5.8	36.66	36.63	16.26	15.15	107.3
.4909	-7.4	34.75	.6302	.5729	-9.1	4.9	36.21	36.21	15.00	14.10	106.4
.4976	1.4	34.8	.5936	.6146	3.5	1.5	36.50	36.43	14.65	14.66	100.3
.5233	-1.9	34.4	.6461	.6080	-5.9	-2.4	36.10	36.07	14.32	13.80	103.8

TABLE I. - Concluded, COMPARISON OF

(b) SI

Run	Ex-pulsion time, sec	Average tank pressure, P_t, av , N/m^2	First segment				Second segment				Third	
			Average liquid-hydrogen temperature, $T_{LH, av}$, $^{\circ}K$	Ideal incremental weight of gaseous helium, $\Delta W_{GHe, id}$, kg	Experi-mental incremental weight of gaseous helium, $\Delta W_{GHe, exp}$, kg	Percentage increase of experi-mental over ideal, η	Average liquid-hydrogen temperature, $T_{LH, av}$, $^{\circ}K$	Ideal incremental weight of gaseous helium, $\Delta W_{GHe, id}$, kg	Experi-mental incremental weight of gaseous helium, $\Delta W_{GHe, exp}$, kg	Percent-age increase of experi-mental over ideal, η	Average liquid-hydrogen temperature, $T_{LH, av}$, $^{\circ}K$	Ideal incremental weight of gaseous helium, $\Delta W_{GHe, id}$, kg
1	77	144.8 $\times 10^3$	20.97	0.0345	0.0424	22.7	20.66	0.0520	0.0577	11.0	20.03	0.0883
2	74	144.4	20.61	.0542	.0634	17.0	20.28	.1279	.0759	2.9	19.89	.2211
3	93	144.5	20.99	.0332	.0450	35.3	20.63	.0545	.0591	8.5	20.25	.0734
4	97	144.3	20.72	.0494	.0618	25.3	20.44	.0662	.0727	9.8	20.00	.0881
5	99	144.8	20.92	.0388	.0439	13.0	20.59	.0569	.0555	-2.5	20.08	.0828
6	102	144.4	20.58	.0576	.0669	16.1	20.27	.0760	.0715	-6.0	19.89	.0961
7	201	144.0	20.98	.0344	.0496	44.1	20.62	.0552	.0622	12.7	20.13	.0826
8	199	144.0	20.61	.0536	.0613	14.3	20.33	.0694	.0717	3.2	20.00	.0908
9	304	143.8	20.97	.0341	.0422	23.6	20.61	.0552	.0619	12.2	20.18	.0811
10	297	144.1	20.67	.0518	.0603	16.3	20.33	.0695	.0733	5.4	19.94	.0934
11	60	171.9	20.82	.0861	.0964	11.9	20.45	.1086	.1049	-3.4	19.88	.1393
12	58	171.9	20.42	.1053	.1080	2.6	20.10	.1197	.1186	-.9	19.56	.1467
13	60	171.7	20.03	.1283	.1329	3.6	19.72	.1457	.1389	-4.7	19.34	.1679
14	98	171.7	21.00	.0772	.0880	14.0	20.67	.0947	.0982	3.7	20.17	.1260
15	97	171.5	20.67	.0933	.1038	11.2	20.33	.1109	.1139	2.7	19.89	.1421
16	97	171.9	20.04	.1300	.1304	.3	19.78	.1442	.1382	-4.2	19.41	.1612
17	198	171.6	21.06	.0755	.0926	22.7	20.61	.1017	.1069	5.1	20.22	.1264
18	198	171.6	20.74	.0928	.1017	9.6	20.43	.1115	.1060	-4.9	20.01	.1339
19	198	171.4	20.16	.1275	.1254	-1.6	19.94	.1403	.1336	-4.8	19.51	.1646
20	299	171.6	21.00	.0799	.1033	29.3	20.61	.1036	.1100	6.2	20.11	.1320
21	300	171.4	20.67	.0989	.1123	13.5	20.28	.1212	.1212	0	19.89	.1450
22	300	171.9	20.06	.1352	.1345	-.5	19.84	.1491	.1401	-6.0	19.47	.1676
23	65	224.4	20.86	.2122	.2448	15.4	20.37	.2088	.2097	.4	19.92	.2251
24	59	227.4	20.58	.1800	.1759	-2.3	20.16	.2113	.1995	-5.6	19.78	.2280
25	96	227.0	20.94	.1688	.1849	9.6	20.56	.1845	.1867	1.2	20.11	.2018
26	94	226.5	20.56	.1797	.1820	1.3	20.22	.1993	.1965	-1.4	19.83	.2393
27	203	227.0	21.04	.1694	.1726	1.9	20.67	.1956	.1834	-6.2	20.22	.2228
28	207	227.5	20.68	.1955	.2063	5.5	20.44	.2139	.2011	-6.0	20.03	.2405
29	297	225.7	21.00	.1719	.1818	5.7	20.61	.1968	.1996	1.4	20.17	.2226
30	306	225.6	20.72	.1886	.1936	2.7	20.39	.2102	.2049	-2.5	20.00	.2420

EXPERIMENTAL RESULTS WITH THEORETICAL IDEAL

units

segment	Fourth segment					Average percentage increase, η_{av}	Average liquid-hydrogen temperature for the entire expulsion, $T_{LH, av}$ °K	Average ullage gas temperature at end of run, $T_{u, av}$ °K	Average experimental gaseous hydrogen pressure for the entire expulsion, $P_{GH, exp}$ N/m ²	Average ideal gaseous hydrogen pressure for the entire expulsion, $P_{GH, id}$ N/m ²	Saturation, ϵ , percent
	Experimental incremental weight of gaseous helium, $\Delta W_{GHe, exp}$ kg	Percentage increase of experimental over ideal, η	Average liquid-hydrogen temperature, $T_{LH, av}$ °K	Ideal incremental weight of gaseous helium, $\Delta W_{GHe, id}$ kg	Experimental incremental weight of gaseous helium, $\Delta W_{GHe, exp}$ kg						
0.0856	-3.0	18.93	0.1434	0.1466	2.2	4.4	20.15	20.26	96.6×10 ³	101.4×10 ³	95.3
.0996	6.9	18.94	.3584	.1408	1.6	5.9	19.93	19.97	89.3	93.1	95.9
.0808	10.1	19.46	.0959	.1023	6.6	11.7	20.33	20.38	100.0	105.4	95.1
.0949	7.6	19.28	.0992	.0997	.5	8.7	20.11	20.15	94.7	97.9	96.7
.0761	-8.1	19.32	.1265	.1173	-7.3	-4.1	20.23	20.25	102.5	101.4	101.1
.0954	-.7	19.16	.1354	.1275	-5.9	-1.1	19.97	19.93	93.8	91.7	102.3
.0898	8.7	19.26	.1271	.1291	1.3	10.4	20.25	20.19	97.4	99.3	98.1
.0968	6.6	19.11	.1343	.1318	-1.9	3.8	20.02	20.05	92.7	95.1	97.4
.0899	10.8	19.35	.1236	.1273	3.0	9.3	20.27	20.21	98.4	100.0	98.4
.0981	5.0	19.11	.1366	.1320	-3.4	3.5	20.02	20.04	92.8	95.1	97.5
.1378	-1.0	19.00	.1834	.1851	.9	1.3	20.04	20.11	94.3	96.9	97.3
.1414	-3.6	18.77	.2024	.1989	-1.8	-1.3	19.71	19.77	86.7	87.2	99.4
.1600	-4.7	18.43	.2096	.1936	-7.6	-4.0	19.38	19.41	81.3	77.9	104.3
.1317	4.6	19.17	.1795	.1734	-3.4	2.9	20.25	20.30	99.5	102.7	96.8
.1432	.8	19.06	.1818	.1838	1.0	3.1	19.99	19.96	91.3	92.4	98.8
.1537	-4.6	18.76	.1944	.1826	-6.1	-4.0	19.49	19.45	84.2	79.3	106.2
.1332	5.4	19.28	.1783	.1757	-1.5	5.5	20.29	20.22	98.8	100.3	98.5
.1263	-5.7	19.26	.1780	.1647	-7.5	-3.4	20.11	20.14	99.7	97.9	101.8
.1529	-7.1	18.90	.1913	.1771	-7.4	-5.6	19.63	19.64	88.7	84.1	105.4
.1384	4.9	19.33	.1748	.1769	1.2	7.8	20.27	20.24	96.7	100.7	96.0
.1466	1.2	19.11	.1850	.1782	3.7	1.5	19.99	19.99	92.7	93.8	98.9
.1573	-6.1	18.89	.1958	.2005	2.4	-5.5	19.57	19.61	86.7	83.1	104.4
.2280	1.3	19.01	.2666	.2693	1.0	4.3	20.04	20.02	92.5	94.8	97.6
.2189	-4.0	18.89	.2776	.2670	-3.8	-4.0	19.86	19.92	95.1	91.4	104.2
.2048	1.5	19.17	.3024	.3020	-.1	2.4	20.19	20.20	96.0	99.3	96.7
.2389	-.2	18.89	.2892	.2831	-2.1	-.8	19.88	19.94	90.9	92.0	98.7
.2070	-7.1	19.54	.2651	.2408	-9.2	-5.8	20.37	20.35	112.1	104.5	107.3
.2227	-7.4	19.31	.2859	.2599	-9.1	-4.9	20.12	20.12	103.4	97.2	106.4
.2257	1.4	19.33	.2693	.2788	3.5	1.5	20.28	20.24	101.0	101.1	100.3
.2374	-1.9	19.11	.2931	.2758	-5.9	-2.4	20.06	20.04	98.7	95.1	103.8

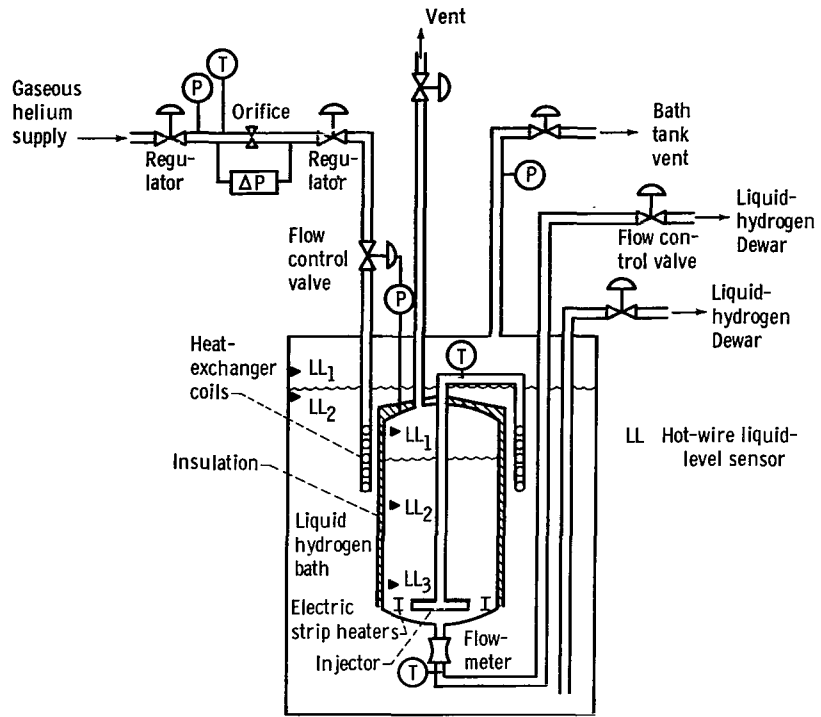


Figure 1. - Test facility.

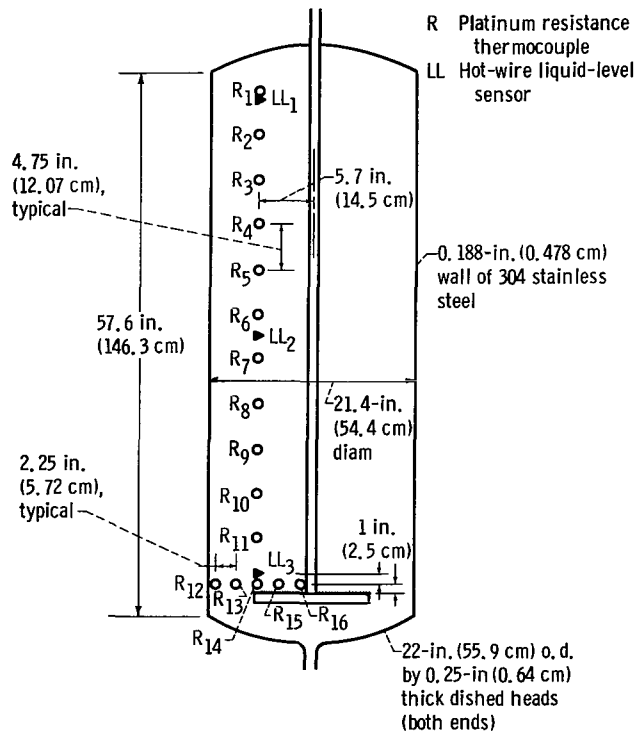


Figure 2. - Test tank and internal instrumentation.

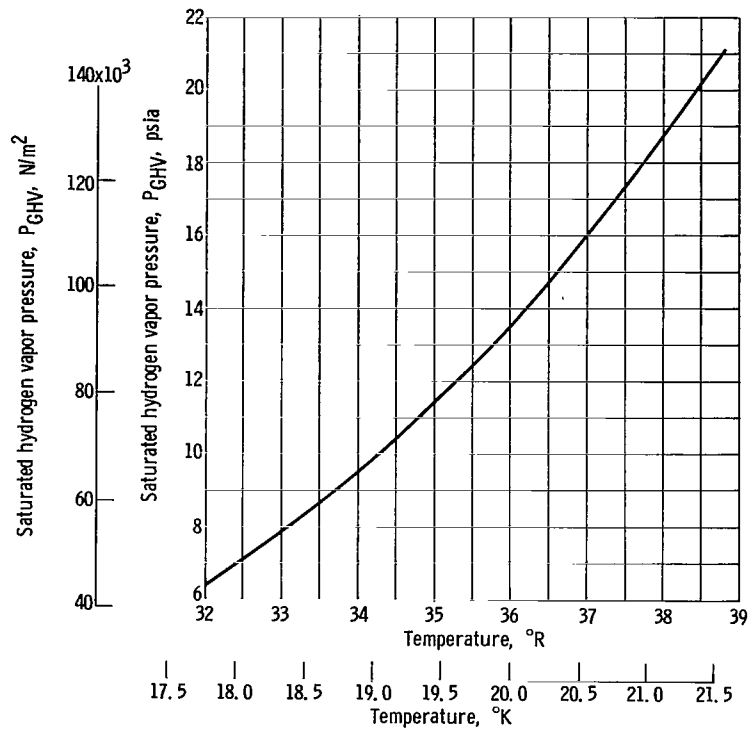


Figure 3. - Saturated vapor pressure of hydrogen as function of temperature.

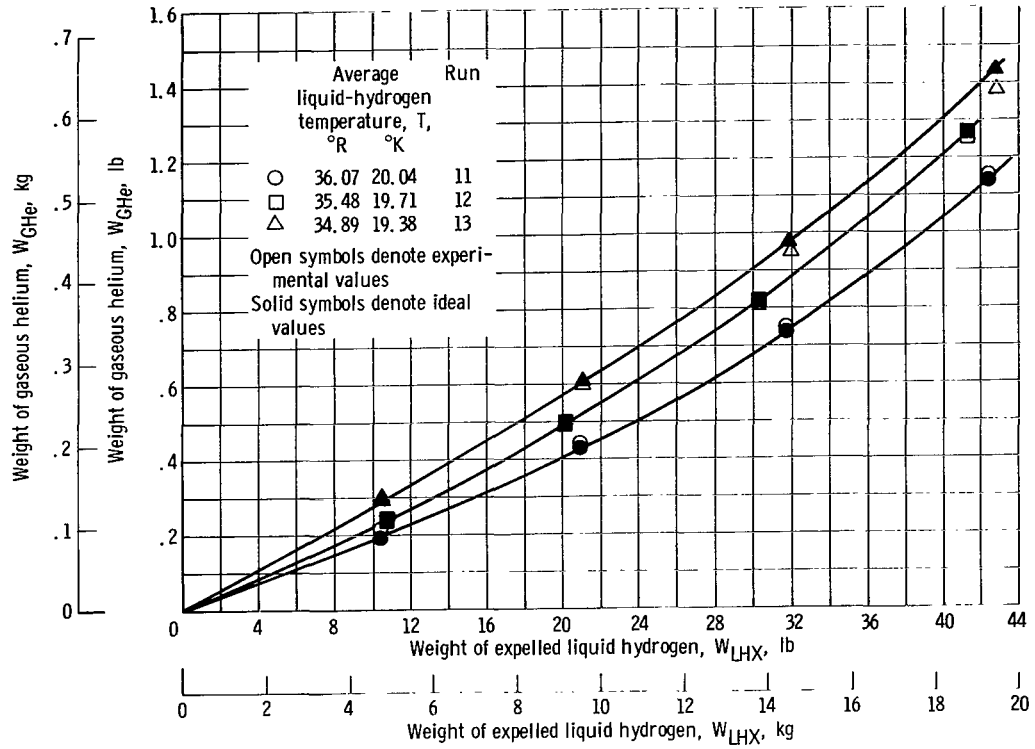


Figure 4. - Comparison of experimental helium pressurant requirements to theoretical ideal for various average liquid-hydrogen temperatures. Tank pressure, 25 psia ($172 \times 10^3 \text{ N/m}^2$); expulsion time, 60 seconds.

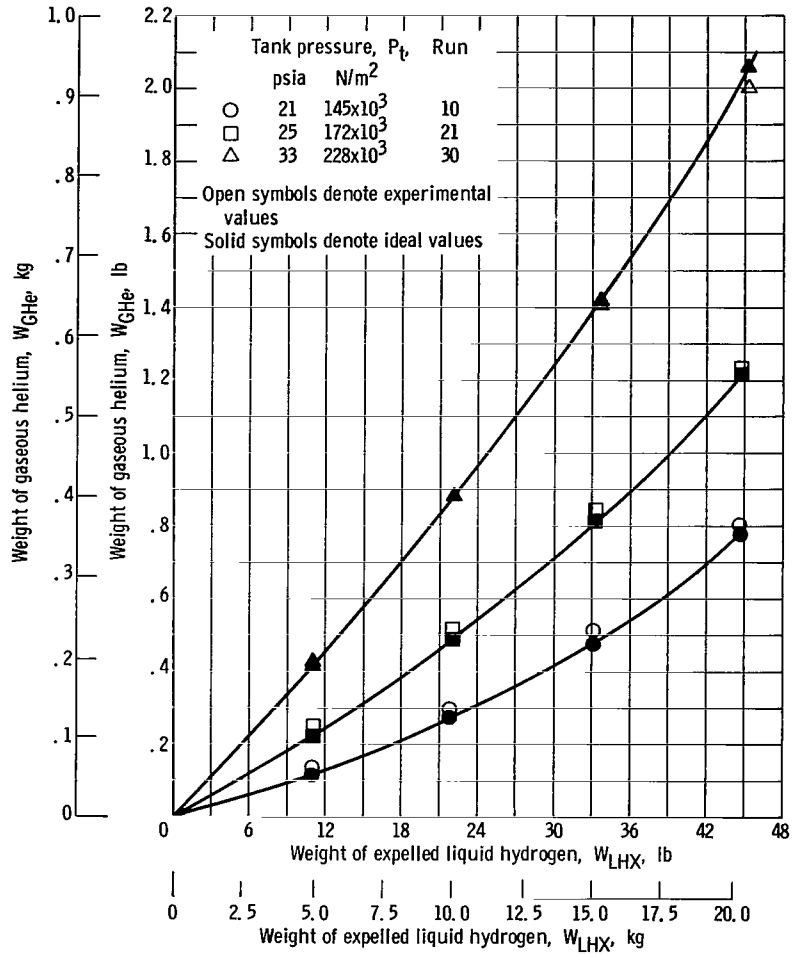


Figure 5. - Comparison of experimental helium pressurant requirements to theoretical ideal for various tank pressures. Average liquid-hydrogen temperature, 37.2° R (20.7° K); expulsion time, 300 seconds.

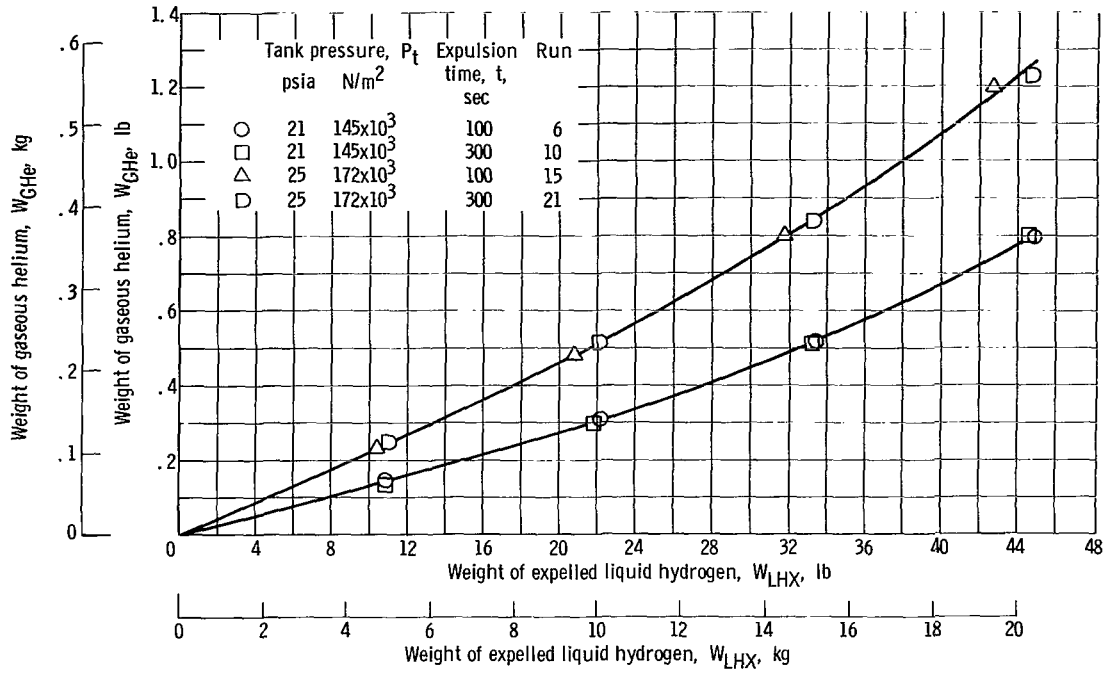


Figure 6. - Effect of various expulsion times on experimental helium pressurant requirements for different tank pressures. Average liquid-hydrogen temperature, 36.0° R (20° K).

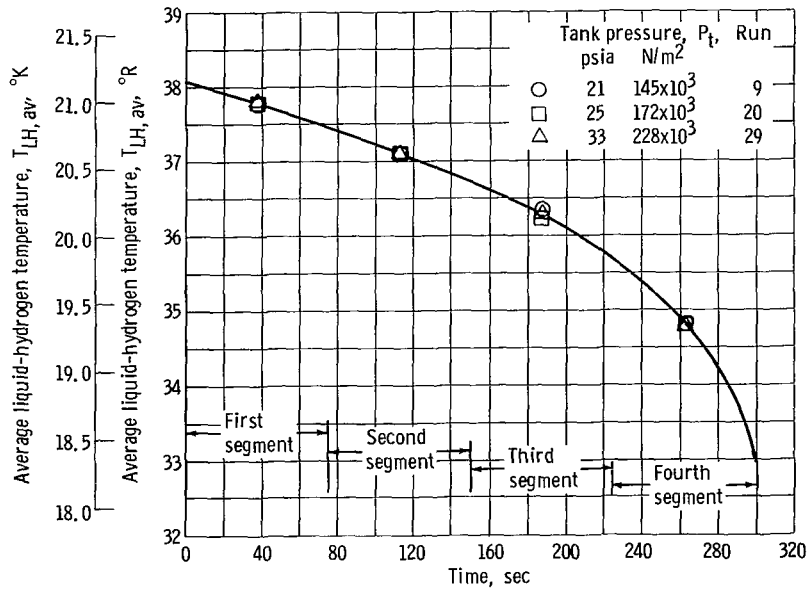
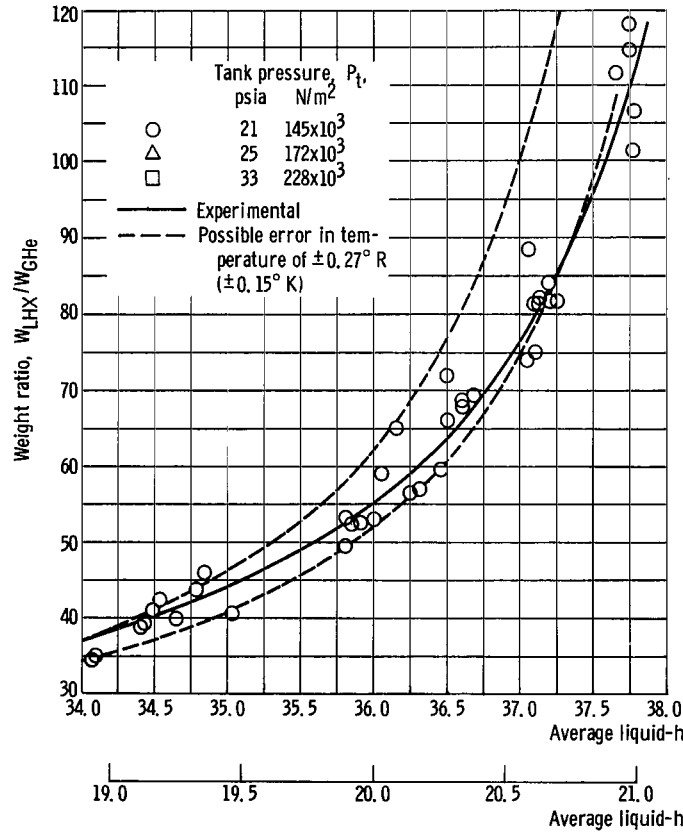
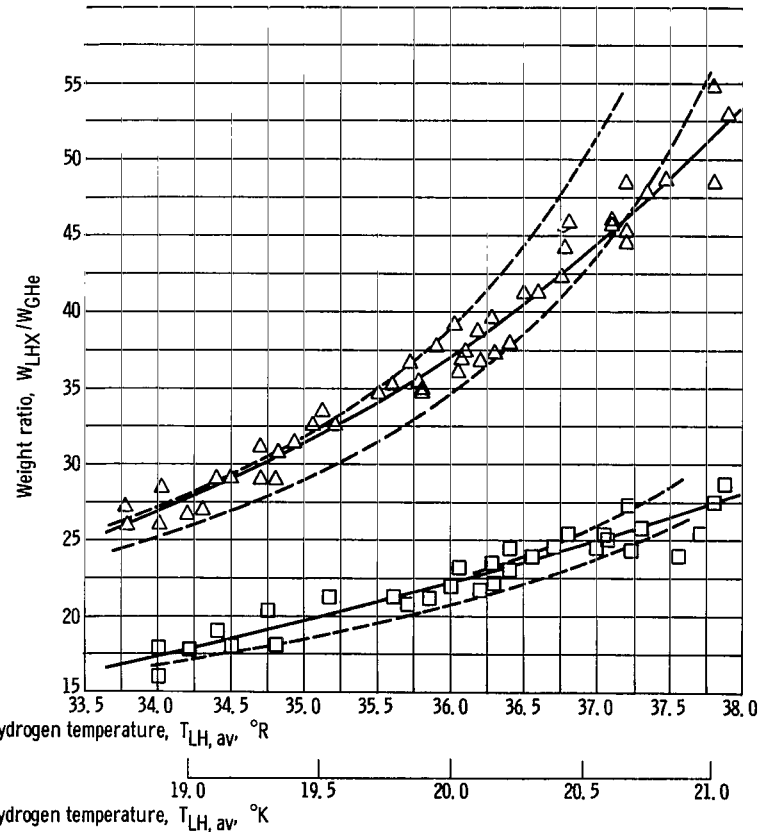


Figure 7. - Average bulk liquid temperature as function of time.



(a) Tank pressure, 21 psia (145×10^3 N/m²).



(b) Tank pressures, 25 and 33 psia (172×10^3 and 228×10^3 N/m²).

Figure 8. - Ratio of pounds of liquid hydrogen expelled per pound of helium pressurant used as function of temperature.

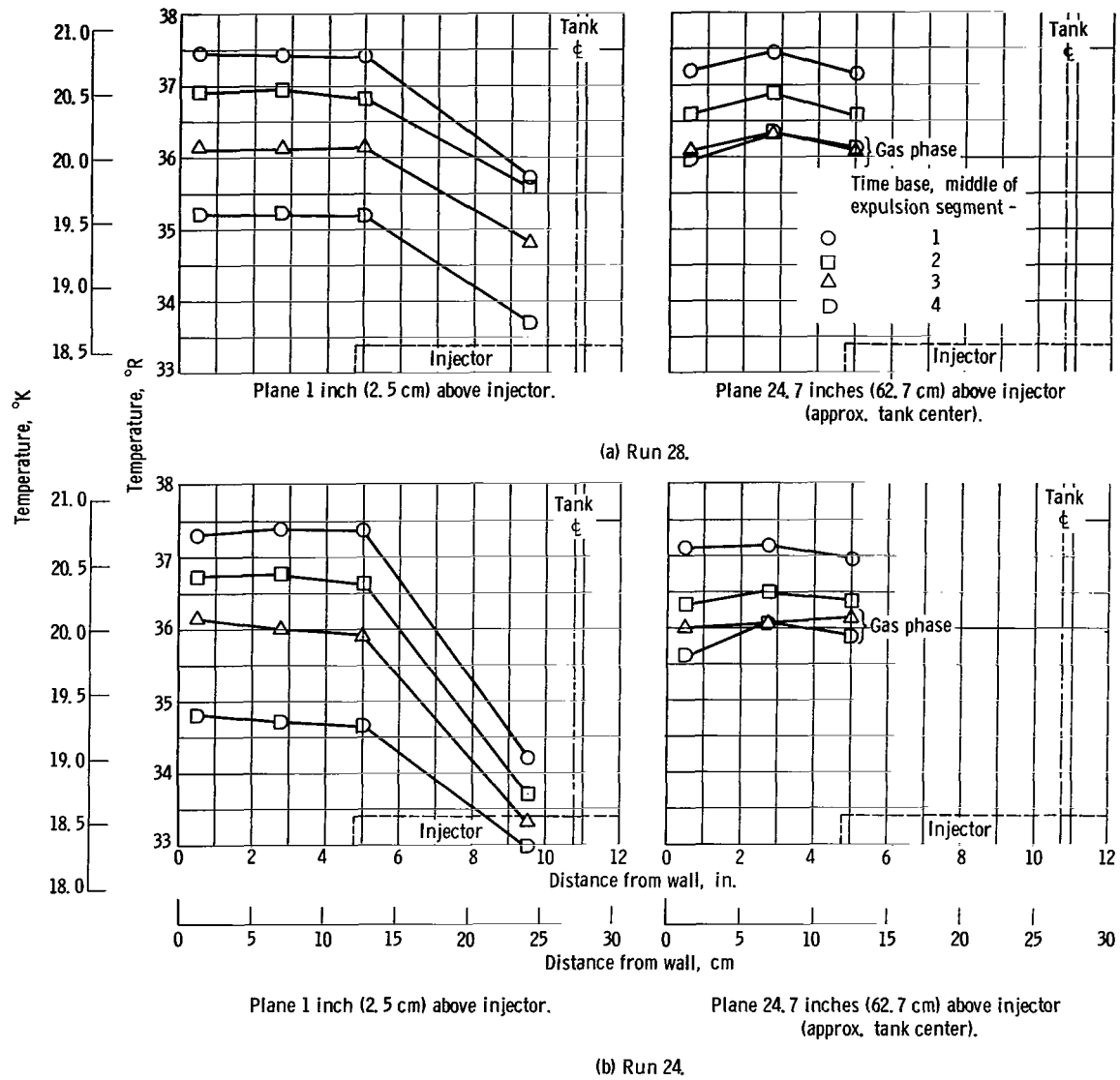


Figure 9. - Radial temperature profiles

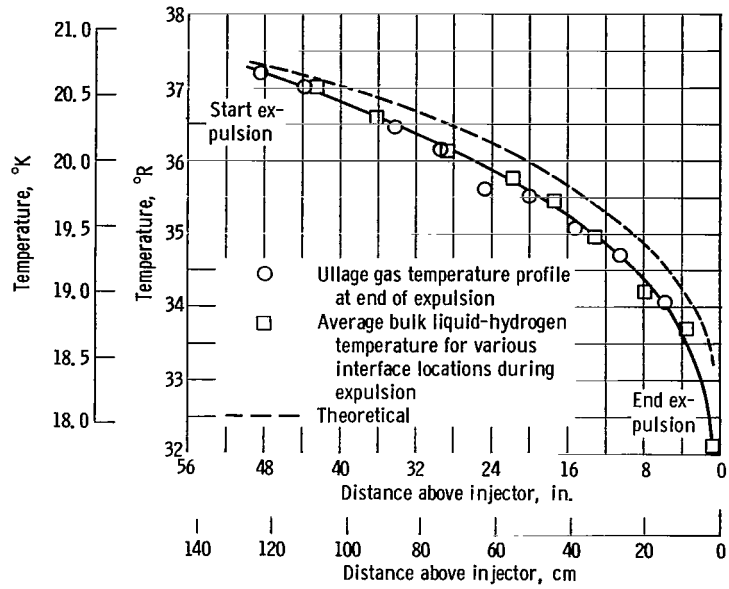
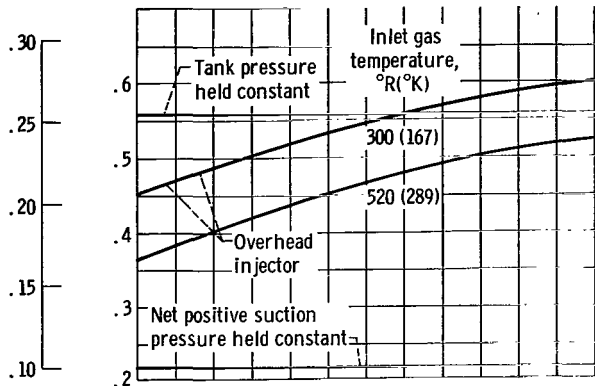
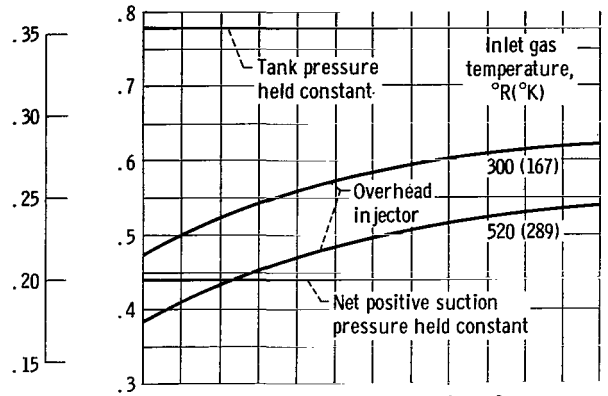


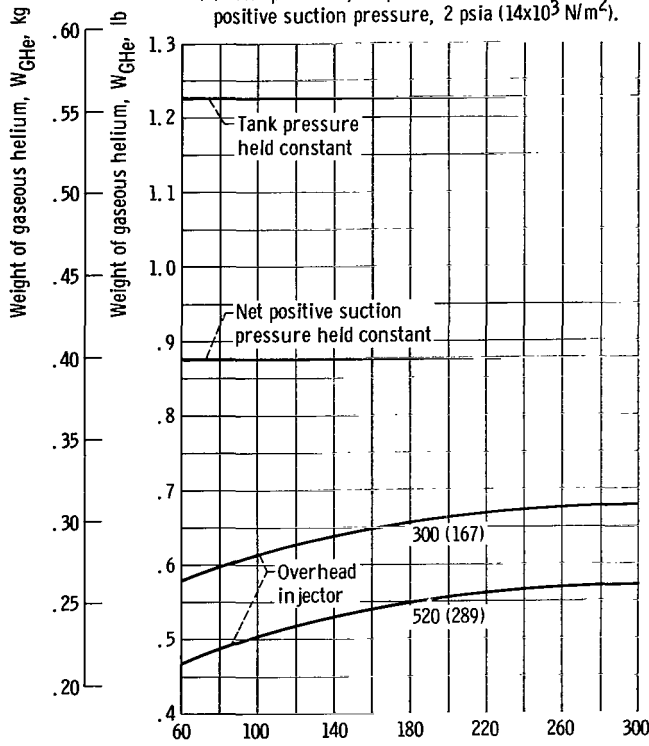
Figure 10. - Comparison of average bulk liquid-hydrogen temperature at various liquid-level heights to final ullage gas temperature profile at end of run 24.



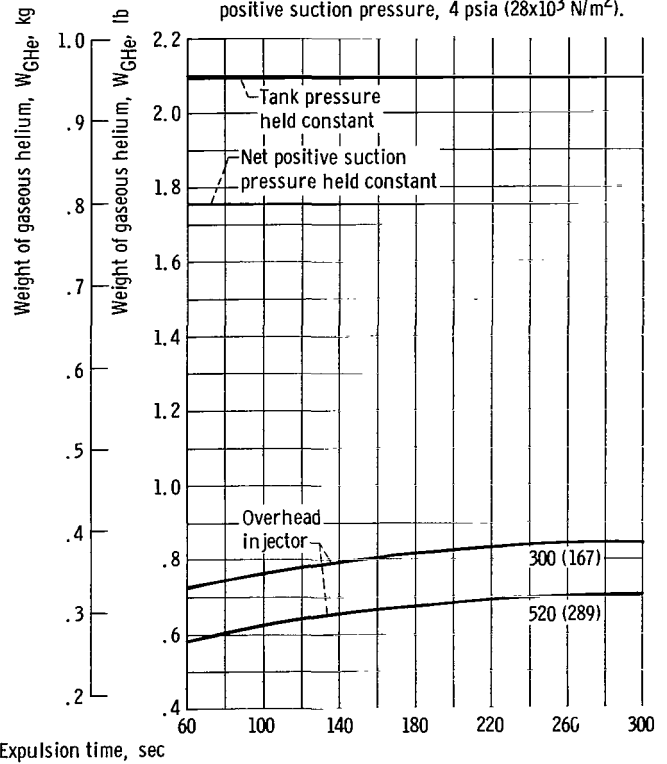
(a) Tank pressure, 19 psia ($131 \times 10^3 \text{ N/m}^2$); net positive suction pressure, 2 psia ($14 \times 10^3 \text{ N/m}^2$).



(b) Tank pressure, 21 psia ($145 \times 10^3 \text{ N/m}^2$); net positive suction pressure, 4 psia ($28 \times 10^3 \text{ N/m}^2$).



(c) Tank pressure, 25 psia ($172 \times 10^3 \text{ N/m}^2$); net positive suction pressure, 8 psia ($55 \times 10^3 \text{ N/m}^2$).



(d) Tank pressure, 33 psia ($228 \times 10^3 \text{ N/m}^2$); net positive suction pressure, 16 psia ($110 \times 10^3 \text{ N/m}^2$).

Figure 11. - Comparison of helium pressurant requirements for submerged injector to those for overhead injector utilizing hot gas.

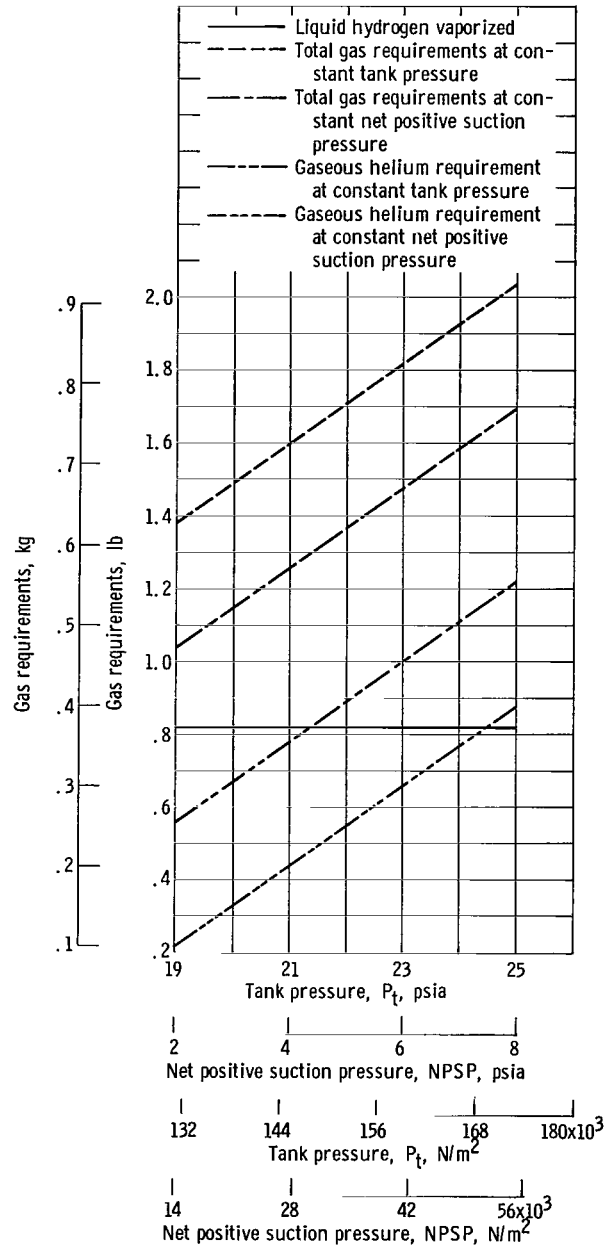


Figure 12. - Gas requirements for submerged injector.

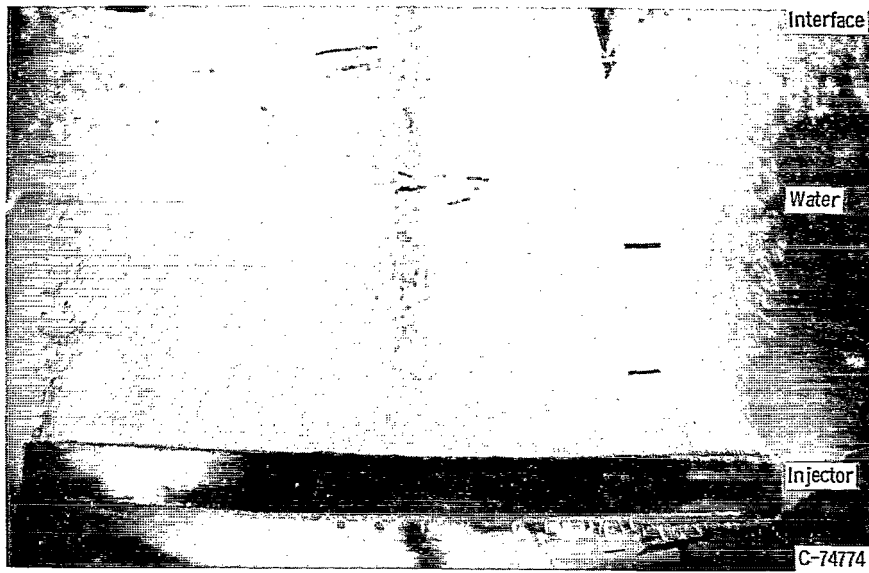


Figure 13. - Helium gas injected into water with injector used in program.

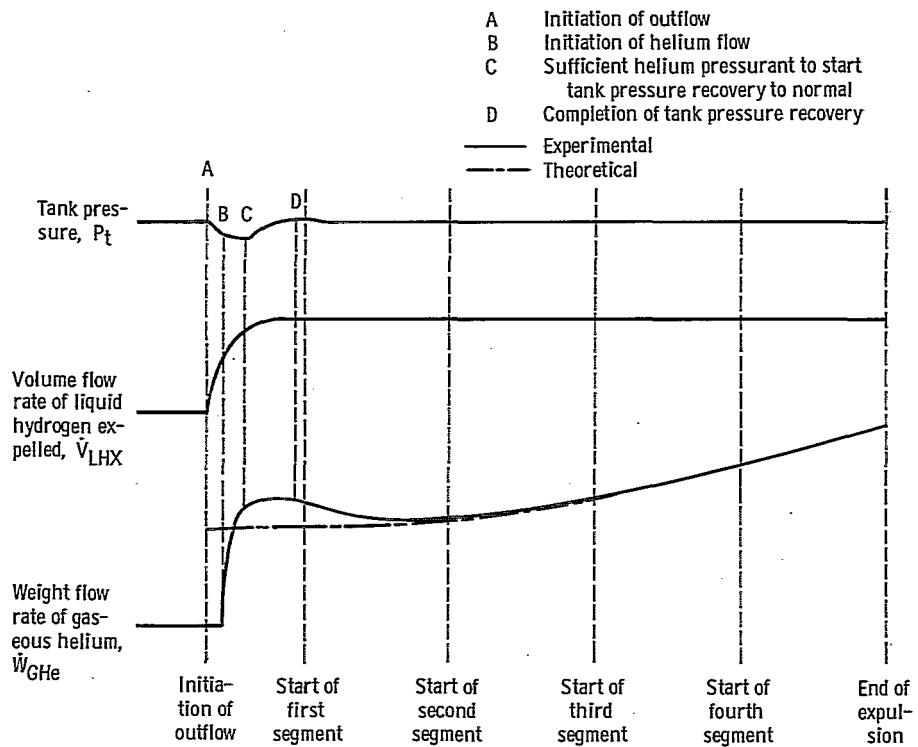


Figure 14. - Typical expulsion profile.

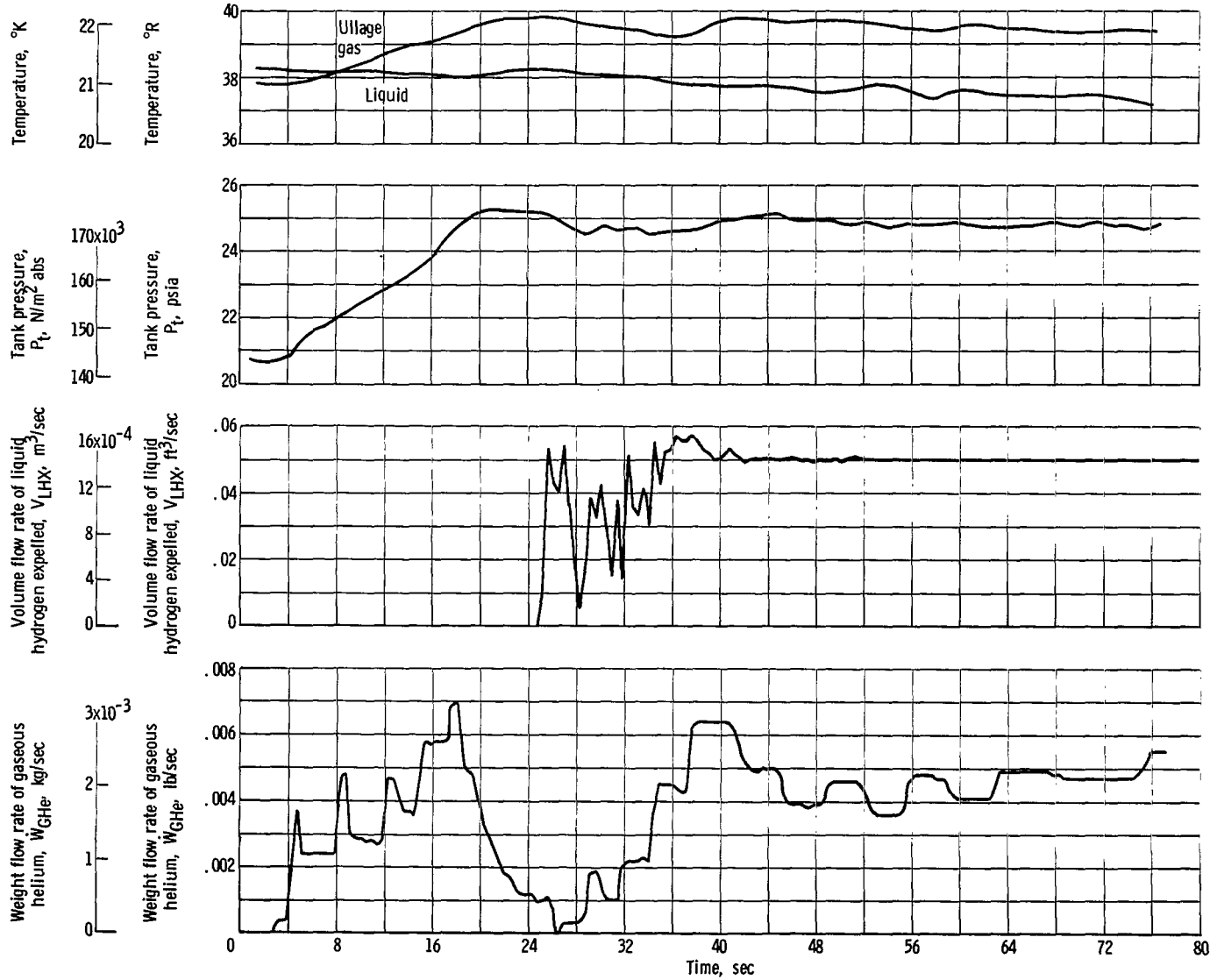


Figure 15. - Temperatures, pressure, and flow rates as functions of time for typical checkout run from start of prepressurization until outflow is established.

"The aeronautical and space activities of the United States shall be conducted so as to contribute . . . to the expansion of human knowledge of phenomena in the atmosphere and space. The Administration shall provide for the widest practicable and appropriate dissemination of information concerning its activities and the results thereof."

—NATIONAL AERONAUTICS AND SPACE ACT OF 1958

NASA SCIENTIFIC AND TECHNICAL PUBLICATIONS

TECHNICAL REPORTS: Scientific and technical information considered important, complete, and a lasting contribution to existing knowledge.

TECHNICAL NOTES: Information less broad in scope but nevertheless of importance as a contribution to existing knowledge.

TECHNICAL MEMORANDUMS: Information receiving limited distribution because of preliminary data, security classification, or other reasons.

CONTRACTOR REPORTS: Scientific and technical information generated under a NASA contract or grant and considered an important contribution to existing knowledge.

TECHNICAL TRANSLATIONS: Information published in a foreign language considered to merit NASA distribution in English.

SPECIAL PUBLICATIONS: Information derived from or of value to NASA activities. Publications include conference proceedings, monographs, data compilations, handbooks, sourcebooks, and special bibliographies.

TECHNOLOGY UTILIZATION PUBLICATIONS: Information on technology used by NASA that may be of particular interest in commercial and other non-aerospace applications. Publications include Tech Briefs, Technology Utilization Reports and Notes, and Technology Surveys.

Details on the availability of these publications may be obtained from:

SCIENTIFIC AND TECHNICAL INFORMATION DIVISION
NATIONAL AERONAUTICS AND SPACE ADMINISTRATION

Washington, D.C. 20546